Gondwana Research 89 (2021) 1–18

Contents lists available at ScienceDirect

Gondwana Research

journal homepage: www.elsevier.com/locate/gr

Updated Antarctic crustal model

A. Baranov [a,*], R. Tenzer [b], A. Morelli [c]

[a] Schmidt Institute of Physics of the Earth, Russian Academy of Sciences, Bol'shaya Gruzinskaya ul, 10, Moscow 123995, Russia
[b] Department of Land Surveying and Geo-Informatics, Hong Kong Polytechnic University, Hong Kong, China
[c] Istituto Nazionale di Geofisica e Vulcanologia, Sezione di Bologna, via Donato Creti 12, 40128 Bologna, Italy

ARTICLE INFO

Article history:
Received 11 November 2019
Received in revised form 3 August 2020
Accepted 6 August 2020
Available online 23 September 2020

Handling Editor: N. Rawlinson

Keywords:
Crustal structure
Sediments
Antarctica
Gondwana

ABSTRACT

We use seismic data together with a subglacial bedrock relief from the BEDMAP2 database to obtain a new three-layer model of the consolidated (crystalline) crust of Antarctica that locally improves the global seismic crustal model CRUST1.0. We collect suitable data for constructing crustal layers, analyse them and build maps of the crustal layer thickness and seismic velocities. We use the subglacial relief according to a tectonic configuration and then interpolate data using a statistical kriging method. The P-wave velocity information from old seismic profiles have been supplemented with the new shear-wave velocity models. We adjust the thickness of crustal layers by multiplying a total crustal thickness by a percentage ratio of each individual layer at each point. Our results reveal large variations in seismic velocities between different crustal blocks forming Antarctica. The most pronounced differences exist between East and West Antarctica. In East Antarctica, a high P-wave velocity ($v_P > 7$ km/s) layer in the lower crust is absent. The P-wave velocity in the lower crust changes from 6.1 km/s beneath the Lambert Rift to 6.9 km/s beneath the Wilkes Basin. In West Antarctica, a thick mafic lower crust is characterized by large P-wave velocities, ranging from 7.0 km/s under the Ross Sea to 7.3 km/s under the Byrd Basin. In contrast, velocities in the lower crust beneath the Transantarctic and Ellsworth-Whitmore Mountains are ~6.8 km/s. The P-wave velocities in the upper crust in East Antarctica are within the range 5.5–6.4 km/s. The upper crust of West Antarctica is characterized by the P-wave velocities of 5.6–6.3 km/s. The P-wave velocities in the middle crust vary within 5.9–6.6 km/s in East Antarctica and within 6.3–6.5 km/s in West Antarctica. A low-velocity layer (5.8–5.9 km/s) is detected at depth of ~20–25 km beneath the Princes Elizabeth Land.

1. Introduction

The continental crust represents the most heterogeneous layer of the Earth's interior that could mask the mantle signature for a variety of geophysical measurements. Knowledge of the crustal structure is therefore important from a point of view of not only understanding the origin and geological history of the lithosphere, but also for a better understanding of processes in the sub-lithospheric mantle. The continental crustal structure varies in thickness, composition, properties and origin, as it represents an assemblage of different terranes with various geological histories (e.g. Christensen and Mooney, 1995). The continental crustal thickness typically varies between 20 and 75 km. The age of the continental crust can exceed 3 Ga in Archean cratons, while the oceanic crust is no older than 200 Ma. During the last few decades, origin, formation and evolution of the continental crust have become the subject of intensive research. Geophysical data provides important clues about its structure and origin. Felsic rocks typically decrease in proportion with depth, while the occurrence of mafic rocks increases. The upper crust is heterogeneous and predominantly felsic. The middle crust (at depths from 10–15 to 20–25 km) is usually intermediate in a bulk composition and composed by amphibolite facies. The lower crust (below 20–25 km) is composed by granulitic rocks with a different composition. It is generally mafic, but can have an intermediate composition in some regions. Large variations in P-wave and S-wave velocities have been detected in the continental crust. These variations are mainly explained by a relatively complex geological structure and age ranging from Achean to Cenozoic. There is an obvious link between the crustal composition and seismic velocity, although there is not a unique correspondence between them (e.g. Tarkov and Vavakin, 1982). A crustal composition can however be inferred using the average P-wave or S-wave velocities from seismic data. Seismic velocities also contribute to knowledge of the crustal density structure, by which parameters of isostatic equilibrium can be derived.

Despite considerable efforts has been undertaken in the last decades to investigate the continental crustal structure, many parts of the world are even now poorly covered by geophysical data. This is particularly true for the Antarctic continent. Consequently, many aspects related to its structure, origin and evolution are not yet fully understood. The

* Corresponding author at: Schmidt Institute of Physics of the Earth, Russian Academy of Sciences, Bol'shaya Gruzinskaya ul, 10, Moscow 123995, Russia.
E-mail address: baranov@ifz.ru (A. Baranov).

https://doi.org/10.1016/j.gr.2020.08.010
1342-937X/

Antarctic continent comprises terranes of different age, from early Archean blocks (Napier craton) to Cenozoic crust in West Antarctica (Bentley, 1991). Crustal blocks of West Antarctica are relatively young (<1.0 Ga), whereas East Antarctica is mainly formed by Proterozoic blocks with the inclusion of Archean blocks (Mikhalsky, 2008). Two main continental rift systems are the East and West Antarctic Rift Systems (Fretwell et al., 2013). This structural variability reflects the origin and tectonic history of the crust and determines its physical properties. Reconstructions and geophysical data revealed the place of Antarctica within the configuration of Gondwana and Rodinia and history of different crustal blocks (Dalziel, 1992). Seismic and gravity datasets have recently been used to study the Moho interface in Antarctica. Seismic data analyses were conducted by Baranov and Morelli (2013) and An et al. (2015). Llubes et al. (2003), Block et al. (2009), Llubes et al. (2017) and Chisenga et al. (2019) used for this purpose gravity data. More advanced studies based on combining seismic and gravity data have been conducted by O'Donnell and Nyblade (2014), Baranov et al. (2018), Shen et al. (2018) and Pappa et al. (2019). The internal crustal structure, involving sediments and underlying crystalline rocks, has also been addressed besides a Moho depth. Pyle et al. (2010) derived a shear wave velocity model for the Transantarctic Mountains and surrounding regions. They identified sediments and a thin crust with a high velocity layer under the Ross Ice Shelf near the Transantarctic Mountains. In East Antarctica, sediments have been detected under the Aurora and Wilkes Basins. Ramirez et al. (2017) derived crustal thickness and shear-wave velocity models for West Antarctica and the Transantarctic Mountains using seismic data from the POLENET/ANET, GSN and TAMSEIS networks. According to their results, the Transantarctic Mountains have an average crustal thickness ~30 km along the front, 38 km in its central part and an average crustal S-wave velocity (v_S) ~3.7 km/s. The Ellsworth Mountains have approximately the same average v_S and a crustal thickness within 35–39 km. The crust under the Marie Byrd Land is ~30 km thick, with the crustal v_S ~3.7 km/s. O'Donnell et al. (2019) estimated the crustal thickness and shear-wave velocity structure for a part of West Antarctica using seismic data from the POLENET/ANET, UKANET and other stations. They detected a very thin crust (22 km) under the Ross Ice Shelf and the Byrd Subglacial Basin. They also inferred a thick crust (36–40 km) beneath the south part of the Transantarctic and Ellsworth Mountains that thins to 30–32 km beneath the Whitmore Mountains. Baranov et al. (2018) developed a model for the Antarctic continental (sedimentary and consolidated) crust based on a joint analysis of gravity and seismic data together with topographic, bathymetric and subglacial relief datasets. They identified large sedimentary basins in West and East Antarctica with a maximum thickness reaching ~14 km under the Filchner-Ronne Ice Shelf. Due to thick sediments, thickness of the consolidated crust in the Antarctic continent (including its continental margins) changes in a wide range from 12 to 16 km beneath the Ronne Ice Shelf to 56 km beneath the Gamburtsev Subglacial Mountains (with an average thickness 31 km). Using the ambient noise tomography and P-wave receiver functions (PRFs), Shen et al. (2018) constructed shear-wave velocity models for West Antarctica, the Transantarctic Mountains and central parts of East Antarctica. They found a thick crust under the Gamburtsev Subglacial Mountains and Vostok Subglacial Highlands (50–56 km). In contrast, they identified a very thin crust (20–28 km) under the Byrd Subglacial Basin and Ross Ice Shelf. Except for studies by Pyle et al. (2010), Ramirez et al. (2017), Shen et al. (2018) and O'Donnell et al. (2019), not much research has been focused to investigate the inner crustal structure. The only continental-scale models containing a three-layer crustal structure are the CRUST2.0 (Bassin et al., 2000) and CRUST1.0 (Laske et al., 2013) global seismic crustal models, but their accuracy in Antarctica is very low. Moreover, these models do not provide information about seismic data coverage. It is thus unknown where these models are based on seismic data and what seismic datasets have been used. Moreover, seismic data obtained after 2013 have not been incorporated in the compilation of CRUST1.0. We also suggest that old deep seismic sounding (DSS) profiles have not been included in CRUST1.0. Large differences between CRUST1.0 and ANTMoho (Baranov et al., 2018) in terms of a thickness of the consolidated crust (from 22 km to 14 km) represent a possibly significant inconsistency in the crustal structure beneath this continent that needs a more careful inspection. When dealing with global crustal seismic models, such as CRUST1.0, the consolidated (crystalline) crust is usually divided into upper, middle and lower crustal layers. We adopted this concept to update a consolidated crustal model for the Antarctic continental crust. Main parameters of crustal layers are depth, thickness, and P and S seismic wave velocities.

In this study, we updated the Antarctic crustal model prepared earlier by Baranov et al. (2018) on the basis of a detailed revision of published seismic results and used this refined information to construct the thickness and P-wave velocity models of the consolidated crust. We used seismic data from profiles and single stations. Some of seismic profiles are little known because they have not been published in English literature. In previous studies, we used them to construct the seismic Moho model (Baranov and Morelli, 2013) as well as the combined (seismic-gravimetric) Moho model (Baranov et al., 2018). In those studies, we focused only on a determination of a Moho depth. Nevertheless, data from seismic profiles and single stations allow us to derive also a three-layer model of the crust with velocities in each layer. The study is organized into five sections and begins with a brief description of the topography, subglacial bedrock relief and tectonic setting of the Antarctic continent in Section 2. Methods and existing seismic datasets are briefly summarized in Sections 3 and 4. The updated crustal model is presented in Section 5. Major findings are discussed and the study is concluded in Section 6.

2. Tectonic setting and subglacial relief

The Antarctic continent (extending over an area of 14×10^6 km^2) is almost entirely (~99%) covered by an ice sheet with a maximum thickness reaching 4.6 km and an average thickness 1.94 km (Fretwell et al., 2013). The surface relief of Antarctica is dominated by its ice dome, rising to the centre of the continent with a maximum thickness up to ~4 km leaving rare bedrock outcrops that can mostly be found near the coast. Maximum topographic elevations reach 4.9 km (Mt. Vinson). The Transantarctic Mountains and the West and East Antarctica Ranges represent the three largest mountains on the continent (Bentley, 1991). The glacial isostatic adjustment due to the current ice load is highly variable ranging from 0 to 1 km. The subglacial relief is very complex, ranging from −2.5 to 4.0 km (Fig. 1) and is on average 79 m below sea level (Fretwell et al., 2013).

The Antarctic continent represents an area of a very high geophysical and tectonic significance because of its unique features. The continent lies almost motionless in the context of global plate tectonic motions, surrounded by the oceanic crust and mainly spreading ridges. It is characterized by an extremely low seismicity. Geologically, it is an assemblage of accreted terranes, making stable platforms as well as tectonically more active regions of continental rifting and orogenic belts. Until now, however, the crustal configuration hidden under the glacial cover has not been fully revealed, although this information is essential for understanding of the tectonic history of each block (Fig. 1). Overall, three different large domains can be recognized within the continent, with ages ranging from Archean to Cenozoic. Most of proposed hypotheses suggest that the present-day geological configuration of Antarctica is the result of four major tectonic events (Kriegsman, 1995; Jacobs et al., 2003; Rino et al., 2008; or Boger, 2011) that began with the stabilization of Archean cratons to Paleoproterozoic blocks (>1.6 Ga), followed by the Grenvillian event that was associated with the formation of the supercontinent Rodinia (1.1 Ga) and its breakup (900–800 Ma). More recent tectonic stages involve the Ross/Pan-African event that is linked to the formation of the supercontinent Gondwana (600–500 Ma) and its breakup (160–100 Ma) that resulted

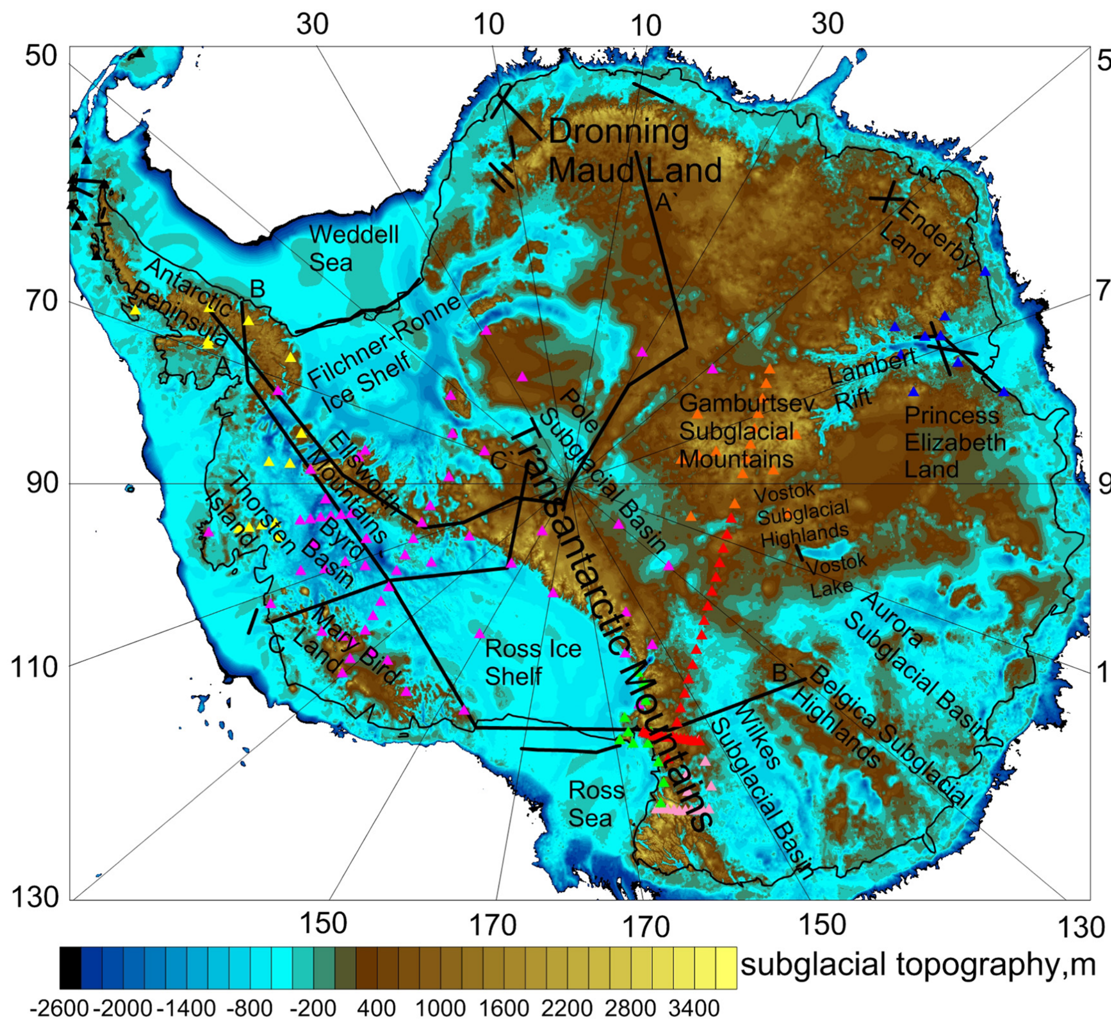

Fig. 1. Tectonic blocks and subglacial relief in Antarctica according to BEDMAP2 (Fretwell et al., 2013). Notation used: black lines represent seismic profiles, red triangles represent the TAMSEIS stations; green triangles represent the GSN stations; yellow triangles represent the UKANET stations; magenta triangles represent the POLENET/ANET stations; orange triangles represent the GAMSEIS stations; blue triangles represent the SSCUA stations; pink triangles represent the TAMNNET stations; and black triangles represent other stations.

in the formation of oceanic basins and the East and West Antarctica Rift Systems.

The Transantarctic Mountains are the largest known non-collisional mountain ranges (ten Brink et al., 1997) without any evidence of a compressional origin (Studinger et al., 2004). This mountain range spans about 3000 km between the Ross Sea and the Wilkes Basin, dividing the continent into East and West Antarctica (Bentley, 1991). West Antarctica is a complex assemblage of accreted terranes of volcanic and magmatic arcs and other crustal blocks with age dating back from Neoproterozoic to Cenozoic. This region represents one of the largest zones of a stretched continental crust in the world (Dalziel and Elliot, 1982). Each crustal block has its own specific geological history. A relative motion of these blocks has been characterized by a prevailing trend towards the East Antarctic Craton during the Gondwana breakup. These processes have been accompanied by stretching of the continental crust and involving mafic magmatic activities (Hole and LeMasurier, 1994). The structure of West Antarctica appears to be more complex than that of East Antarctica. It involves the Ross Sea Embayment, the Marie Byrd Land with the Bentley Depression, the Ellsworth-Whitmore Mountains, the Antarctic Peninsula and the Filchner-Ronne Ice Shelf with the Weddell Sea region (Wörner, 1999).

The West Antarctic Rift System separates the Transantarctic Mountains from the Marie Byrd Land (Behrendt et al., 1991; Winberry and Anandakrishnan, 2004; Chaput et al., 2014). Analysing rock outcrops, Mikhalsky (2008) suggested that East Antarctica is dominantly a Precambrian crustal block composed of different, mainly Proterozoic, terranes. Nevertheless, a large glacial cover (up to 4 km in thickness) is a major factor that restricts understanding of the geology and tectonic history of East Antarctica especially in its central part. East Antarctica could be divided into several geological units comprising the Dronning Maud Land, the Enderby Land, the Prince Charlez Mountains, the Lambert Rift, the Gamburtsev Subglacial Mountains, the South Pole region, the Princess Elizabeth Land, the Aurora Basin, the Vostok Basin and the Wilkes Basin. Tectonically, East Antarctica is categorized into three main blocks of the Indo-Antarctic and Australo-Antarctic segments and the central East Antarctic Craton (e.g. Fitzsimons, 2000; Reading, 2006). East Antarctica is formed primarily by Archean, Proterozoic and early Palaeozoic rocks. It includes several Archean cratons and Proterozoic terranes with a different geological history. Several crustal terranes in East Antarctica are possibly formed by ancient rocks. The Grunehogna, Mawson and Napier Cratons preserved evidences of tectonic activities from Archean (Baranov and Bobrov, 2018). Archean rocks have also been identified south of the Prince-Charlez Mountains, parts of the Princes Elizabeth Land and in the Adelie Land (Mikhalsky, 2008). The crust of East Antarctica was formed mainly in Archean and later reworked during the Proterozoic orogeny (Paleoproterozoic, Grenville and Pan-African events) with an intense tectono-thermal activation (Bentley, 1973).

The Dronning Maud Land consists of several crustal blocks ranging in age from Archean to early Palaeozoic. The Maudheim Province is an eastern extension of the Namaqua-Natal-Belt in Africa (1.2–1.0 Ga). The Archean Grunehogna Craton (3.4–3.0 Ga) is located in the Atlantic sector of East Antarctica in the west part of the Dronning Maud Land and is surrounded by the Maudheim Province. According to paleo-reconstructions (Jacobs et al., 1998), the Grunehogna Craton formed part of the Kaapvaal Craton until the Jurassic breakup of Gondwana followed by the separation of this craton from the Kaapvaal Craton (Groenewald et al., 1991). The Pan-African Orogeny (500–600 Ma) is another major event that formed several orogenic structures in the Dronning Maud Land, particularly the Sor Rondane Mountains and the Wohlthat Massif. These structures possibly represent a southern extension of the East African Orogen into East Antarctica (Jacobs et al., 1998). There is a pronounced suture zone between the Grunehogna Craton and Maudheim Province (Bayer et al., 2009). Ancient rocks forming the central Dronning Maud Land underwent a strong high-grade reworking during the Pan-African event (600–500 Ma). The Kottas Mountains are interpreted to be a remnant of an island arc (1.1–1.0 Ga) (cf. Bayer et al., 2009).

The Enderby Land formed during the breakup of east margins of India and East Antarctica. The Lutzow-Holm Complex is a part of the Pan-African Mobile Belt in Antarctica, whereas the Rayner Complex and the northern part of the Prince Charles Mountains are an extension of the Eastern Ghats of India. Lambert Rift extends inside East Antarctica more than 700 km from the coast to the Gamburtsev Mountains, with a possible extension around the Gamburtsev Mountains towards the South Pole region, forming the East Antarctic Rift System. The rift is bounded by the Prince Charles Mountains to the west and by the Princess Elizabeth Land to the east. It is filled by sediments up to 6 km thick. This rift was formed during the breakup of East Gondwana (Boger and Wilson, 2003; Lisker et al., 2003). Filina et al. (2008) suggested that the Vostok Basin is possibly a part of the East Antarctic Rift System (see also Isanina et al., 2009; Ferraccioli et al., 2011).

A large region characterized by a low bedrock topography between the Princess Elizabeth Land and the Transantarctic Mountains forms the Aurora and Wilkes Basins that are divided by the Belgica Subglacial Highlands (Aitken et al., 2014). These areas with a low subglacial topography possibly form the Australo-Antarctica block, whereas the regions situated to the west form the Indo-Antarctica block. The Aurora Subglacial Basin is characterized by a low and smooth subglacial topography, sediments and thinned crust. The Wilkes Basin is a broad area with a negative subglacial relief (Fretwell et al., 2013) and thinned crust (Lawrence et al., 2006) due to a flexural response to the Transantarctic Mountains uplift (ten Brink et al., 1997), or to processes associated with a continental rifting (Ferraccioli et al., 2001). Sediment infills in these basins reach thickness of several kilometres (Baranov et al., 2018).

The Gamburtsev Subglacial Mountains are located in the central part of East Antarctica and are fully covered by ice. Their origin is uncertain. Hansen et al. (2010) speculated that these mountains could be an old orogeny associated with Proterozoic or Palaeozoic events with a later reactivation. Ferraccioli et al. (2011) justified the subglacial relief as a possible result of the combined effect of rift-flank uplift, root buoyancy and isostatic response to erosion. The final formation of East Antarctica occurred only at the turn of Proterozoic and Palaeozoic, as the result of amalgamation of Archean and Proterozoic terranes (Reading, 2006). The basement of East Antarctica comprises various rocks (Mikhalsky, 2008), most notably the Early Archean enderbites, charnockites and granite-gneisses (3.8–4.0 Ga), Archean-Early Proterozoic granite-gneisses of the amphibolite facies, late Archean-Early Proterozoic metasomatic charnockites, intrusive charnockitoids (2000–500 Ma) and Palaeozoic granites (500–360 Ma).

3. Methods

The Moho depth and the depth to the basement are among parameters most reliably determined from seismic data. Seismic data can also be used to define inner crustal margins. The definition of inner crustal margins is, however, more complicated because different methods can provide different stratifications in the same region. Moreover, not all seismic datasets are suitable for this purpose. The best resolution for inner crustal boundaries is often obtained from reflection profiles (Kanao et al., 2011). The velocity information can also be obtained from Deep Seismic Sounding (DSS), wide-angle reflection and refraction profiles with intermediate resolution (1–2 km). Another technique that became quite common during the last decades is based on inverting the so-called receiver functions (RF), either as the P-wave receiver functions (PRFs) (e.g. Zhu and Kanamori, 2000; Ramirez et al., 2017) or the S-wave receiver functions (SRFs) (e.g. Reading, 2006; Hansen et al., 2009, 2016). These methods provide a velocity profile at a point. Other researchers used the Rayleigh and Love wave phase and group velocities (Pyle et al., 2010; Hansen et al., 2010; O'Donnell et al., 2019). Ramirez et al. (2017) and Shen et al. (2018) combined the Rayleigh wave phase and group velocities with PRFs.

Our Antarctic crustal model was constructed by collecting all seismic data that contain information about the inner crustal structure. For each initial data array, whether a seismic profile or array of RFs, we distinguished three layers of the consolidated crust and calculated a thickness of crustal layers as a percentage of the total crustal thickness. In this study, we calculated the P-wave velocity from the S-wave velocity profiles using the ratio $v_P/v_S = 1.73$ according to the IASP91 model (Kennett and Engdahl, 1991). We divided the consolidated crust into three layers to ensure consistency with CRUST1.0. It should be noted that among all the data types used to construct a Moho map only some are suitable for modelling the internal crustal structure and for estimating seismic velocities. Therefore, our technique for the construction of an integrated unified map differs in some details from techniques used for a Moho recovery. The basis of our maps was the BEDMAP2 (Fretwell et al., 2013) subglacial relief (Fig. 1). We then assembled velocities and thicknesses of crustal layers resulting from seismic data analyses. The seismic data sources are shown in Figs. 2 and 3 (see also Tables 1 and 2). The resulting data distribution for the whole continent is quite irregular, with large areas where seismic data are sparse or absent (Fig. 1). In the case of disagreement between different data, we preferred data with a better estimated accuracy. The idea behind this method was to reproduce trends estimated by combining initial seismic data and additional contours according to the subglacial bedrock relief. After that, we interpolated all six resulting data arrays (the P-wave velocities and thicknesses of crustal layers) into uniform grids using a spherical equidistant projection. The result of this procedure is represented by six maps of the P-wave velocity in the upper, middle and lower crust together with the individual thicknesses of crustal layers. This modelling strategy had been used before to build Moho maps for Antarctica (Baranov and Morelli, 2013; Baranov et al., 2018) and the crustal model for Central and Southern Asia (Baranov, 2010). Obviously, with an increasing distance between observed seismic data the reliability of data interpolation decreases. A thickness model for the solid crust has been built using the combined seismic-gravimetric Moho model and our sediment model obtained from seismic and BEDMAP2 data (Baranov et al., 2018). This sediment model fits well with the recently published and completely independent sediment model for surrounding oceanic areas (Straume et al., 2019). Due to the fact that a relative ratio of the thickness of individual layers varies more smoothly than their absolute thicknesses, we interpolated a relative thickness of consolidated crustal layers with respect to the total thickness. Hence, we first interpolated a relative thickness of upper and middle portions of the consolidated crust, while the thickness of the bottom layer was determined to reach 100% of crustal thickness.

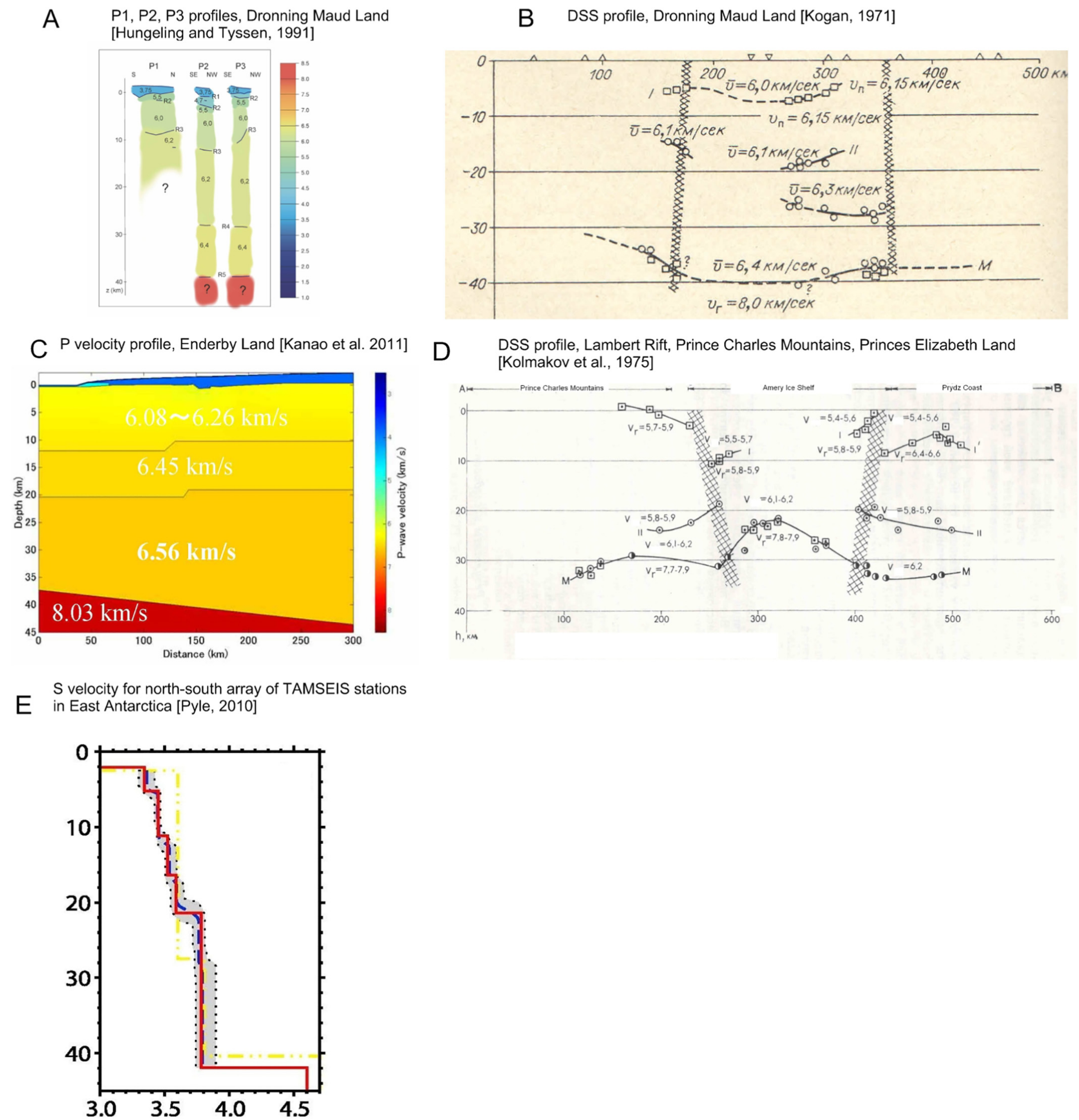

Fig. 2. Seismic data for East Antarctica. A: The P2 and P3 profiles from Hungeling and Tyssen (1991), B: the Novo profile from Kogan (1971), C: the SEAL2000 profile from Kanao et al. (2011), D: the AB profile from Kolmakov et al. (1975), E: the S-velocity diagram from the TAMSEIS north-south profile (Pyle et al., 2010).

These results have been transformed into absolute values by multiplying them with a total thickness of the consolidated crust at each point.

The area covered by our crustal model is the whole Antarctic continent, bordered by the coastline (Fig. 1). For each map (of the thicknesses and P-wave velocities in the upper, middle and lower crust), we created a grid on a mesh 1° × 1° constructed by applying an azimuthal equidistant projection. We then interpolated data using a standard kriging technique with a linear variogram (SURFER, Golden Software package). The scale was set one. The variogram was intended to find a local neighbourhood of any observed point and to weight values from observed points with an interpolating function to find the value a given grid point. The goal of this geostatistical method is to reproduce trends estimated from seismic data alone. The kriging parameters were chosen as follows: the interpolation area was from the South Pole to 60°S, the grid step was 1° on a geographical latitude-longitude grid with no anisotropy. We trimmed the grid at a border of the Antarctic continent. It was indeed quite difficult to estimate uncertainties of a model that has been obtained by merging different types of data that often do not carry any accuracy information themselves. Unfortunately, for many grid

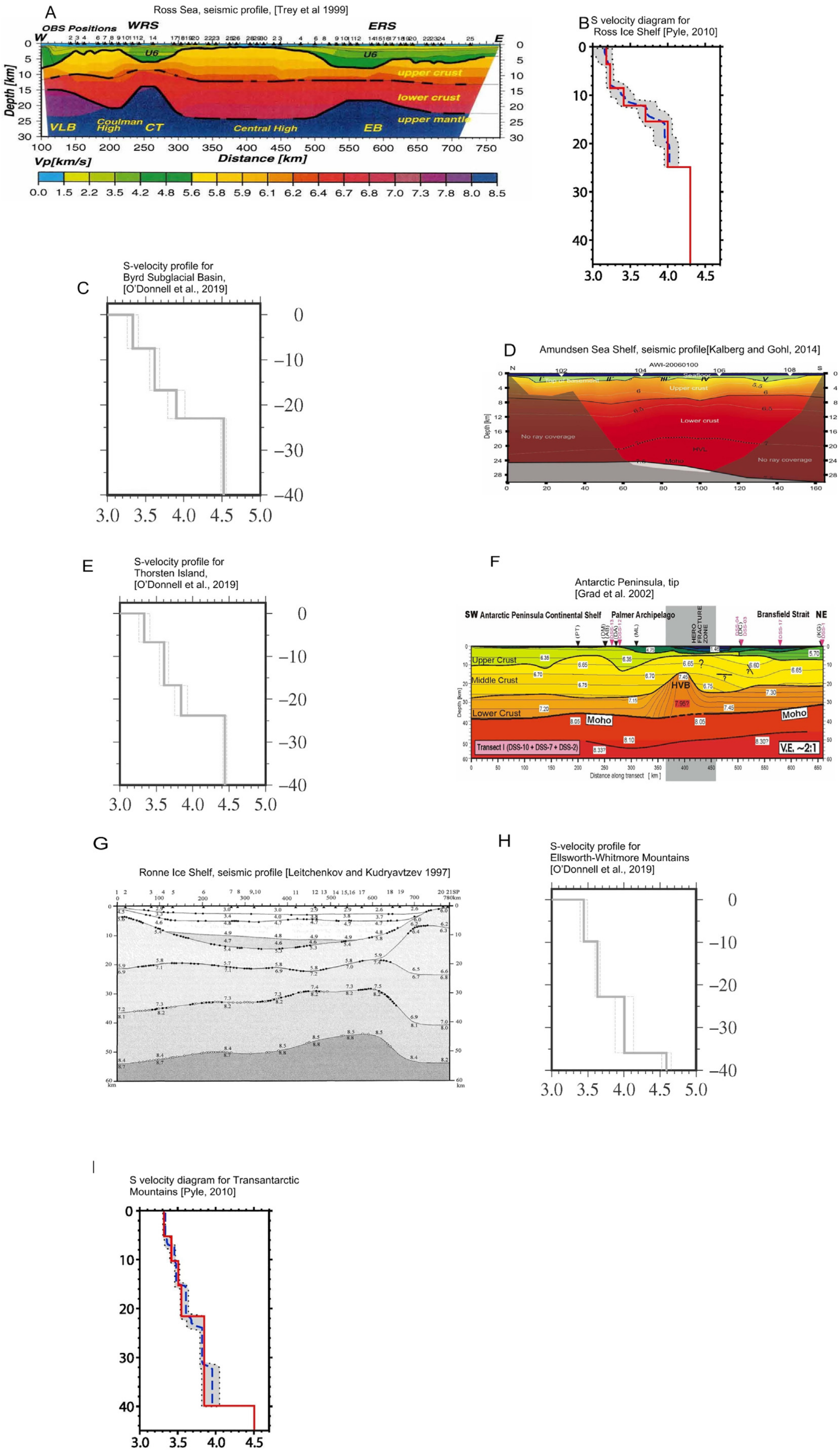
A
Ross Sea, seismic profile, [Trey et al 1999]
OBS Positions
WRS
ERS
W
E
U6
upper crust
lower crust
upper mantle
VLB
Coulman High
CT
Central High
EB
Depth [km]
Distance [km]
Vp[km/s]
0.0 1.5 2.2 3.5 4.2 4.8 5.6 5.8 5.9 6.1 6.2 6.4 6.7 6.8 7.0 7.3 7.8 8.0 8.5
B
S velocity diagram for Ross Ice Shelf [Pyle, 2010]
C
S-velocity profile for Byrd Subglacial Basin, [O'Donnell et al., 2019]
D
Amundsen Sea Shelf, seismic profile[Kalberg and Gohl, 2014]
Upper crust
Lower crust
No ray coverage
HVL
Moho
E
S-velocity profile for Thorsten Island, [O'Donnell et al., 2019]
F
Antarctic Peninsula, tip [Grad et al. 2002]
SW Antarctic Peninsula Continental Shelf
Palmer Archipelago
HERO FRACTURE ZONE
Bransfield Strait
NE
Upper Crust
Middle Crust
Lower Crust
HVB
Moho
Transect I (DSS-10 + DSS-7 + DSS-2)
V.E. ~2:1
Distance along transect [km]
G
Ronne Ice Shelf, seismic profile [Leitchenkov and Kudryavtzev 1997]
H
S-velocity profile for Ellsworth-Whitmore Mountains [O'Donnell et al., 2019]
I
S velocity diagram for Transantarctic Mountains [Pyle, 2010]

Table 1
Summary of seismic data for Antarctica. For each data specified are the: reference, type, Moho, sediments, crustal and sediments structure and region.

Source	Type	Moho (km)	Sediments	Crustal structure	Sediment structure	Region	Additionally
Kogan, 1971	DSS profile	34–40	–	+	–	Dronning Maud Land	Published for the first time in English literature
Bentley, 1973	Three long seismic refraction profiles	–	+	Partly	–	AA profile: Antarctic Peninsula – Dronning Maud Land, BB profile: Antarctic Peninsula – Victoria Land CC profile: Marie Byrd Land–Transantarctic Mountains	These profiles provide information mainly for sediments and upper crust
Kolmakov et al., 1975	Two DSS profiles	24–34	-	+	-	Lambert Rift, Prince Charles Mountains, Princes Elizabeth Land	Published for the first time in English literature
McGinnis et al., 1985	Reflection profiles	20–30	–	partly	–	Ross Sea near Ross Island	
Hungeling and Tyssen, 1991	3 seismic profiles	40	+	+	–	Dronning Maud Land	
Jokat et al., 1996	Refraction and reflection profiles	30–40	+	+	+	Filchner-Ronne Ice Shelf	A group of profiles along the coast from Antarctic Peninsula to Berkner Island
Leitchenkov and Kudryavtzev, 1997	DSS profile	30–40	+	+	+	Filchner-Ronne Ice Shelf	Long profile across the main tectonic structures of the Filchner-Ronne Ice Shelf from the border of the East Antarctica to Antarctic Peninsula
Trey et al., 1999	Seismic profile	16–24	+	+	+	Ross Sea	Long profile across the main tectonic structures of the Ross Sea
Grad et al., 2002	20 refraction profiles	30–40	+	+	+	Near the coast of the Antarctic Peninsula	
Winberry and Anandakrishnan, 2004	Receiver functions	20–30	–	–	–	West Antarctica	
Reading, 2004	S receiver functions	30–40	–	+	–	East Antarctica	DRV and Casey stations on the coast.
Reading, 2006	S receiver functions	30–42	–	+	–	Lambert Rift, Prince Charles Mountains, Princes Elizabeth Land	
Bayer et al., 2009	Receiver functions, refraction profile	32–52	–	+ (partly)	–	Dronning Maud Land	Vp/Vs for some stations, crustal structure for profile
Isanina et al., 2009	Converted waves	32–36	+	Partly	–	Vostok Basin	
Hansen et al., 2010	S receiver functions, Rayleigh wave phase velocities	40–58	–	–	–	Gamburtsev Mountains and surroundings	
Pyle et al., 2010	S receiver functions	20–40	+	+	–	Transantarctic Mountains, Wilkes Basin and surroundings	
Kanao et al., 2011	Two DSS profiles	36–40	–	+	-	Enderby Land	
Kalberg and Gohl, 2014	Two refraction profiles	24–30	+	+	–	Near the coast of the Marie Byrd Land	
Chaput et al., 2014	P-to-S Receiver functions	18–45	+	–	–	West Antarctica, Transantarctic Mountains	
Hansen et al., 2016	S receiver functions	20–46	–	–	–	Transantarctic Mountains and surroundings	
Ramirez et al., 2017	S receiver functions and Rayleigh wave velocities	24–40	–	+	–	West Antarctica, Transantarctic Mountains and surroundings	
Shen et al., 2018	P receiver functions and ambient noise	20–56	–	+	–	Gamburtsev Mountains and surroundings, part of West Antarctica and Transantarctic Mountains	
O'Donnell et al., 2019	Seismic ambient noise	22–40	+	+	–	West Antarctica	The map of crustal radial anisotropy

points we only had one data source, so we had no possibility to evaluate their uncertainties. Nevertheless, we observed some regional details in maps of the P-wave velocities and crustal layers which are absent in CRUST1.0 and CRUST2.0 (Figs. 6, 8).

4. Seismic data

The seismic data used for the analysis of inner crustal structure are summarized in Tables 1 and 2. For a data collection purpose, we divided

Fig. 3. Seismic data for West Antarctica and the Transantarctic Mountains. A: the ACRUP seismic profile for Ross Ice Shelf (Trey et al.,1999), B: the S-velocity profile for the Ross Ice Shelf region (Pyle et al., 2010), C: the S-velocity profile for Byrd Subglacial Basin (O'Donnell et al., 2019), D: the AWI profile for Marie Byrd Land (Kalberg and Gohl, 2014), E: the S-velocity profile for Thorsten Island (O'Donnell et al., 2019), F: the DSS-10, DSS-7 and DSS-2 profiles for the Antarctic Peninsula (Grad et al.,2002), G: the DSS profile for Filchner-Ronne Ice Shelf (Leitchenkov and Kudryavtzev, 1997), H: the S-velocity diagram for the Ellsworth-Whitmore Mountains (O'Donnell et al., 2019), I: the S-velocity diagram for the Transantarctic Mountains (Pyle et al., 2010).

Table 2
Consolidated crust: structure and origin. P-wave velocities that are derived from S-wave velocities using the ratio $v_P/v_S = 1.73$ are marked by an asterisk.

Region	Total thickness, km	Upper crust, km	Middle crust, km	Lower crust, km	Upper crust, Vp, km/s	Middle crust, Vp, km/s	Lower crust, Vp, km/s	Structure and origin, Vp/Vs	Age
Dronning Maud Land (Hungeling and Tyssen, 1991; Kogan, 1971; Bayer et al., 2009)	30–50	8–16	11–18	10–17	6.0	6.1–6.2	6.4	Kottas Mountains: remnant arc of paleosubduction (1.72). Grunehogna Archean craton: granitic gneisses, (1.82). Sor-Rondane and Wohlthat Mountains (1.67): Pan-African event, granitic rocks. Maudheim Province: gneisses (1.72): Grenville event.	1.1–1.0 Ga 3.4–3.0 Ga 500–600 Ma 1.1 Ga
Enderby Land (Kanao et al., 2011)	36–40	8–10	13–14	14–15	6.1–6.2	6.4	6.6	Lutzow-Holm complex: Pan-African event Napier Archean Craton (granulites, charnokites); Rayner complex: Grenville event, highgrade granulite facies gneiss, with charnockite intrusions.	500–600 Ma 3.4–4.0 Ga 1.1–1.0 Ga
Lambert Rift, Prince Charles Mountains, Princes Elizabeth Land (Kolmakov et al., 1975; Reading, 2006)	20–26 34–40 34–38	6–10 10–12 10–12	6–8 12–14 10–13	6–8 12–13 12–13	5.4–5.6 5.7–5.9 5.4–5.6	5.8–5.9 5.8–5.9 5.8–6.6	6.1–6.2 6.1–6.2 6.2	Gondwana break-up, high grade granulite facies Origin is unknown; gneisses, granulites, charnockitoids and metamorphic rocks. Part of Kuunga Suture? Paragneisses and granite gneisses. Grove Mountains – gneisses and granites.	Palaeozoic-Mezozoic Archean-Proterozoic Archean-Proterozoic
Gamburtsev Subglacial Mountains and Vostok Subglacial Highlands (Hansen et al., 2010; Shen et al., 2018)	44–56	14–18	14–18	14–18	6.2–6.6*	6.6–6.7*	6.7–6.9*	Origin is unknown, no rock samples	Proterozoic orogenic event?
Vostok Basin (Filina et al., 2008; Isanina et al., 2009)	24–30	8–10	8–10	8–10	–	–	–	The break-up of Gondwana? No rock samples	160–100 Ma?
Pole Subglacial Basin (Shen et al., 2018)	30–36	10–12	10–12	10–12	6.1–6.2*	6.2–6.4*	6.4–6.7*	Origin is unknown, no rock samples	?
Aurora Basin and Adventure Trough (Aitken et al., 2014)	28–30	10	10	10	–	–	–	The break-up of Gondwana? No rock samples	160–100 Ma?
Belgica Subglacial Highlands (Aitken et al., 2014)	30–36	10	10	10–12	–	–	–	Origin is unknown, no rock samples	?
Wilkes Subglacial Basin (Bentley, 1973; Pyle et al., 2010; Shen et al., 2018)	26–30	8–10	8–10	8–10	5.8–6.2*	6.2–6.6*	6.6–6.9*	Uplift of Transantarctic Mountains? No rock samples	?
Transantarctic Mountains (Bentley, 1973; Pyle et al., 2010; Hansen et al., 2016; Shen et al., 2018)	32–44	10–14	10–14	12–16	6.1–6.2*	6.2–6.6*	6.6–6.9*	Flexural uplift or thermal mechanisms. Sedimentary rocks lying upon a basement of granites and gneisses	1.6–0.9 Ga
Ross Ice Shelf (Trey et al., 1999; Pyle et al., 2010; Hansen et al., 2016; Shen et al., 2018)	12–23	4–7	4–8	4–8	5.9–6.2*	6.4–6.7*	6.9–7.1*	Part of West Antarctic Rift System, Mezozoic-Cenozoic extension, no rock samples	?
Byrd Subglacial Basin (Bentley, 1973; Shen et al., 2018; O'Donnell et al., 2019)	12–20	4–8	4–6	4–6	5.9–6.2*	6.4–6.6*	7.3*	Part of West Antarctic Rift System, Mesozoic-Cenozoic extension, no rock samples	?
Marie Byrd Land (Kalberg and Gohl, 2014; Ramirez et al., 2017; Shen et al., 2018; O'Donnell et al., 2019)	24–30	8–10	8–10	8–10	5.5–6.2*	6.0–6.6*	6.5–7.4*	Volcanic uplifted plato? Granodiorites and granites.	1500–100 Ma
Antarctic Peninsula, end (Grad et al., 2002)	30–38	10–12	10–13	10–13	6.3–6.4	6.7	7.2	Marine sediments.	358–65 Ma
Antarctic Peninsula, base (Bentley, 1973; Shen et al., 2018; O'Donnell et al., 2019)	32–38	10–12	10–13	12–13	6.1–6.2*	6.4–6.6*	7.3*	Marine sediments.	358–65 Ma
Thorsten Island (Shen et al., 2018; O'Donnell et al., 2019)	18–22	6	6–8	6–8	6.2–6.4*	6.4–6.6*	7.1–7.4*	?	?
Filchner-Ronne Ice Shelf near the coast (Leitchenkov and Kudryavtzev, 1997; Jokat et al., 1996)	12–32	4–14	4–10	4–8	5.3–5.9	6.4–6.5 (for border with East Antarctica)	7.1–7.4	Part of West Antarctic Rift System? Mesozoic-Cenozoic extension, deep sedimentary basin, no rock samples	?
Filchner-Ronne Ice Shelf near the Ellsworth Mountains (Shen et al.,	14–32	4–10	4-10	6–12	6.1–6.2*	6.2–6.4*	6.6–7.4*	Part of West Antarctic Rift System? Mesozoic-Cenozoic extension, deep sedimentary basin, no rock samples	?

Table 2 (*continued*)

Region	Total thickness, km	Upper crust, km	Middle crust, km	Lower crust, km	Upper crust, Vp, km/s	Middle crust, Vp, km/s	Lower crust, Vp, km/s	Structure and origin, Vp/Vs	Age
2018)									
Ellsworth-Whitmore Mountains (Shen et al., 2018; O'Donnell et al., 2019)	30–38	10–12	10–12	10–14	6.1–6.2*	6.2–6.4*	6.6–6.9*	Part of Transantarctic Mountains?	?

the whole continent into the following tectonic blocks: the Dronning Maud Land, the Enderby Land, the Prince Charles Mountains, the Lambert Rift, the Prince Elizabeth Land, the Gamburtsev Mountains, the Vostok Basin, the Aurora Basin, the Belgica Subglacial Highlands, the Wilkes Basin, the Transantarctic Mountains, the Ross Ice Shelf, the Byrd Subglacial Basin, the Marie Byrd Land, the Thorsten Island, the Antarctic Peninsula, the Filchner-Ronne Ice Shelf, the Ellsworth-Whitmore Mountains and other regions. These blocks are characterized by a different age, tectonic and geological structure. Seismic profiles, unlike receiver functions, give information about a crustal structure along their entire length. We paid attention to old DSS profiles that were forgotten because they provide important information about a crustal structure beneath large regions where other seismic data are sparse or missing. We processed data from seismic profiles, recent PRF sand SRFs, the Rayleigh and Love wave phase and group velocities to appraise stratification of the consolidated crust (Figs. 2, 3).

4.1. East Antarctica

For the Dronning Maud Land, seismic profiles P2 and P3 from Hungeling and Tyssen (1991) and the Novo profile from Kogan (1971) revealed the low P-wave velocities 6.0, 6.1–6.2 and 6.4 km/s, respectively in the upper, middle and lower crustal layers (Fig. 2a, b). Note that we used this order of crustal layers hereafter for identifying respective velocities. These profiles are rather similar although the P2 and P3 profiles belong to the Grenville Maudheim Province (1.1 Ga), while the Novo profile belongs to the East African Antarctic Orogen (550 Ma). For the Enderby Land, we used data from two seismic profiles for a territory near the coast (Kanao et al., 2011). The P-wave velocities are 6.1–6.2, 6.4 and 6.6 km/s (Fig. 2c). The SEAL2000 profile is located along the border between the East African Antarctic Orogen and the Grenvillian Rayner Complex (i.e. E-W Gondwana suture). In 1971, two DSS profiles (AB and additional CD) were carried out across the Lambert Rift and surrounding regions (Kolmakov et al., 1975). The AB profile is very important because it crosses three different terranes, particularly the Prince Charlez Mountains, the Lambert Rift and the Princess Elizabeth Land (Fig. 2d). Its northern section across the Prince Charlez Mountains is characterized by a two-layer crust with a thick upper crust (5.7–5.9 km/s) and a thin lower crust (6.1–6.2 km/s). For the Lambert Rift, the three-layer crustal model is characterized by the P-wave velocities 5.6, 5.8 and 6.2 km/s. The Princess Elizabeth Land is an Archean-Proterozoic terrane with a low-velocity zone at depth ~20 km. For this crustal block, the P-wave velocities are 5.4–5.6, 5.8–6.6 and 6.2 km/s. Such low velocities in the lower crust for terranes of East Antarctica are also observed in other parts of the world. As examples we could mention the Basin and Range Province (6.6 km/s), the Rheingraben (6.25 km/s), the Kenya Rift (6.6 km/s), the Dead Sea (6.6 km/s), or the Alps (6.3–6.4 km/s; Rudnick and Fountain, 1995). We note here that seismic profiles for the Lambert Rift (Kolmakov et al., 1975) and for the Dronning Maud Land (Kogan, 1971) were published in English for the first time here. For the Lambert Rift region there are also SRFs from the SSCUA deployment (Reading, 2006). Shear wave velocity models derived by receiver functions beneath stations near DSS profiles relatively closely agree with velocity models along such profiles, except at the FISH station. For our model, we used SRFs data from stations located far from seismic profiles, inland in the Princess Elizabeth Land along the Mawson Escarpment (stations GROV and NMES), the Southern Prince Charlez Mountains (station CRES) and along the coast (the station MAW; Reading, 2006). We also used SRFs from two stations near the coast of East Antarctica (Reading, 2004). The seismic profile for the Vostok Basin only provides a thickness of sediment and crustal layers (Isanina et al., 2009). Some recent SRFs are located in other provinces of East Antarctica. The GAMSEIS array of stations provides information about a shear wave velocity under the Gamburtsev Subglacial Mountains and the Vostok Subglacial Highlands, where the S-wave velocities are 3.6–3.8, 3.8–3.9 and 3.9–4.0 km/s (Shen et al., 2018). Under the Wilkes Subglacial Basin, the S-wave velocities are 3.5–3.6, 3.6–3.8 and 3.8–4.0 km/s (Shen et al., 2018). These values agree with previous studies by Pyle et al. (2010) and Hansen et al. (2016). The continuation of the Wilkes Basin to the South Pole (i.e. the Pole Subglacial Basin) has the S-wave velocities 3.5–3.6, 3.6–3.7 and 3.7–3.9 km/s (Shen et al., 2018). Fig. 2e shows the S-wave velocity profile for this part of East Antarctica.

4.2. West Antarctica

The Ross Ice Shelf is a broad region characterized by a low subglacial topography. It is part of the West Antarctic Rift System, formed by a stretched continental crust. The P-wave velocity models from seismic profiles (Trey et al., 1999; McGinnis et al., 1985) reveal rather a high velocity ~7.0 km/s for the lower crustal layer, whereas the upper crust has a low velocity (5.9–6.0 km/s; Fig. 3a). Recent studies (Shen et al., 2018) reported the crustal shear wave velocities 3.4–3.6, 3.7–3.9 and 4.0–4.1 km/s. These values agree with estimates from seismic profiles and the shear wave velocity model for the Ross Sea near the Transantarctic Mountains prepared by Pyle et al. (2010; Fig. 3b). In our study, we adopted these values. The Byrd Subglacial Basin is a continuation of the Ross Ice Shelf along the Transantarctic Mountains, with a very low subglacial topography. Shen et al. (2018) provided the shear wave velocity model for this region with values 3.5–3.7, 3.7–3.8 and ~4.2 km/s for each crustal layer. This model closely agrees with the model derived independently by O'Donnell et al. (2019). Fig. 3c shows the average S-wave velocity profile for the Byrd Subglacial Basin. Subglacial depressions of the Ross Ice Shelf and the Byrd Basin closer to the coast of West Antarctica turn into the Marie Byrd Land with a rather high bedrock topography. For the Marie Byrd Land, the AWI-20060100 seismic profile near the coast (Fig. 3d) provides the P-wave velocities 5.5–6.0 km/s in the upper crust, 6.0–6.5 km/s in the middle crust and 7.0–7.4 km/s in the lower crust (Kalberg and Gohl, 2014). Nearby, but already ashore, the CC′ profile presents the P-wave velocities ~6.1 km/s in the upper crust. A more recent shear wave velocity model for the central part of the Marie Byrd Land shows the S-wave velocities of 3.5–3.6, 3.7–3.8 and 3.9–4.2 km/s (Shen et al., 2018). For the Thorsten Island region, Shen et al. (2018) provided the shear wave estimates 3.6–3.7, 3.7–3.8 and 4.1–4.3 km/s. These values agree with O'Donnell et al. (2019). Fig. 3e shows the average S-wave velocity profile for the

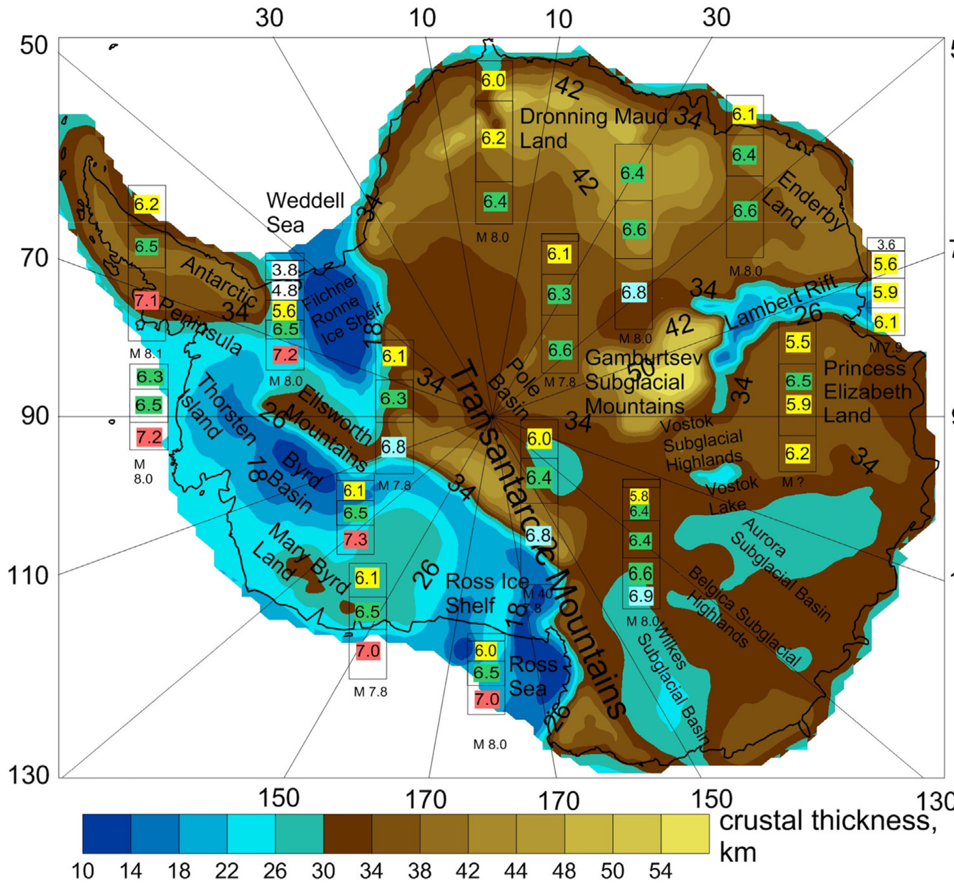
Dronning Maud Land
Weddell Sea
Antarctic Peninsula
Filchner Ronne Ice Shelf
Enderby Land
Lambert Rift
Gamburtsev Subglacial Mountains
Princess Elizabeth Land
Thorsten Island
Ellsworth Mountains
Byrd Basin
Pole Basin
Transantarctic Mountains
Vostok Subglacial Highlands
Vostok Lake
Aurora Subglacial Basin
Mary Byrd Land
Ross Ice Shelf
Belgica Subglacial Highlands
Wilkes Subglacial Basin
Ross Sea
crustal thickness, km
10 14 18 22 26 30 34 38 42 44 48 50 54

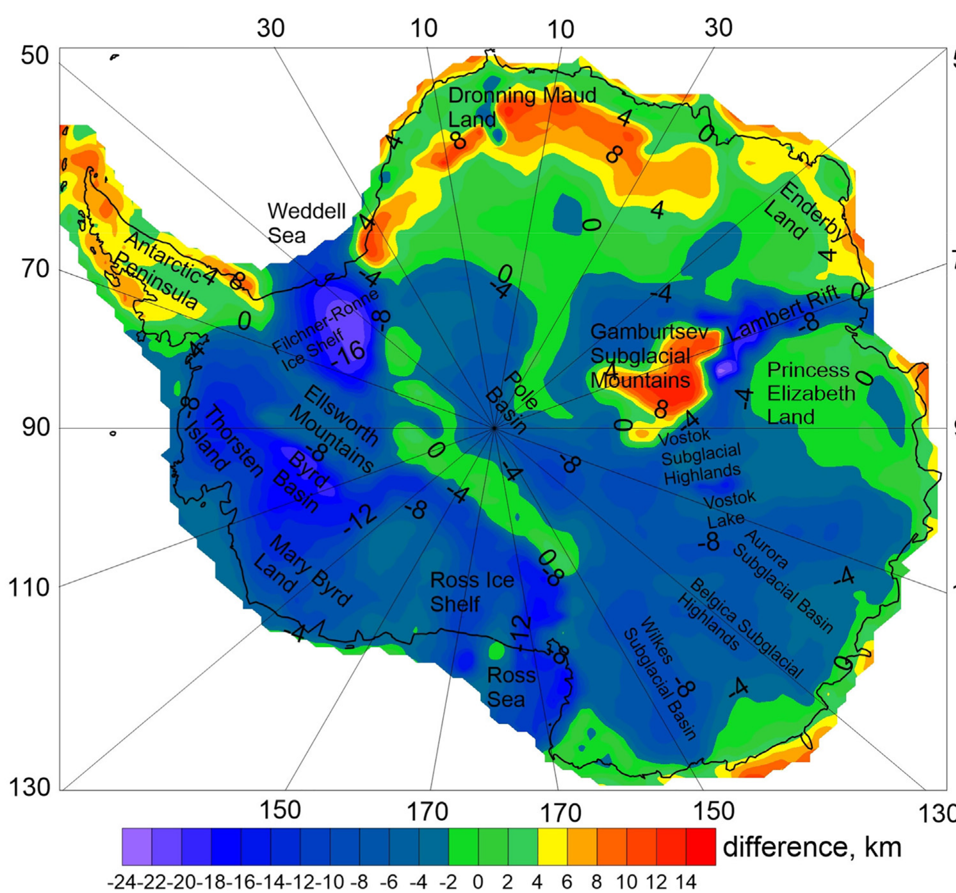
Dronning Maud Land
Weddell Sea
Enderby Land
Antarctic Peninsula
Filchner-Ronne Ice Shelf
Lambert Rift
Gamburtsev Subglacial Mountains
Princess Elizabeth Land
Pole Basin
Thorsten Island
Ellsworth Mountains
Byrd Basin
Vostok Subglacial Highlands
Vostok Lake
Aurora Subglacial Basin
Mary Byrd Land
Ross Ice Shelf
Belgica Subglacial Highlands
Wilkes Subglacial Basin
Ross Sea
difference, km
-24 -22 -20 -18 -16 -14 -12 -10 -8 -6 -4 -2 0 2 4 6 8 10 12 14

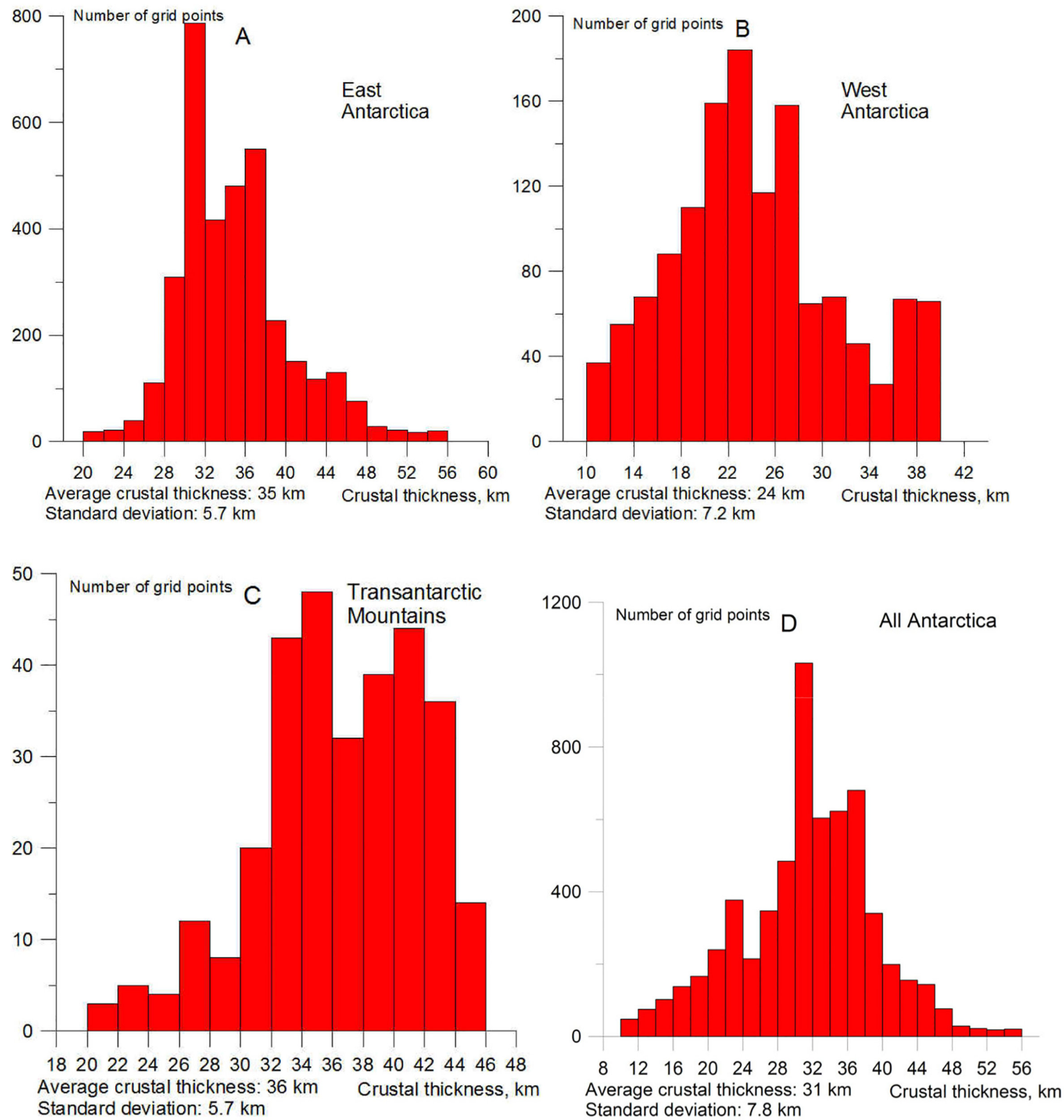

Fig. 5. Histograms of the consolidated crustal thickness for East Antarctica, West Antarctica, the Transantarctic Mountains and for the whole continent.

Thorsten Island. For the tip of the Antarctic Peninsula and near its coast, the three-layer crustal model is characterized by the P-wave velocities 6.3–6.4, 6.7 and 7.2 km/s (Grad et al., 2002) (Fig. 3f). For the base of the Antarctic Peninsula, the shear wave model provides the S-wave velocities 3.5–3.6, 3.7–3.8 and 3.9–4.2 km/s (Shen et al., 2018; O'Donnell et al., 2019). For the upper crust, these values correspond with results obtained from the seismic profiles AA′ and BB′. At the Filchner-Ronne Ice Shelf, a large subglacial basin situated between the Antarctic Peninsula and East Antarctica characterized by low bedrock topography, crustal properties change along the DSS profile near the coastline. The easternmost part of the Filchner-Ronne Ice Shelf is an example of a typical continental crust with the P-wave velocities 6.0–6.2, 6.4–6.5 and 6.8–7.0 km/s (Leitchenkov and Kudryavtzev, 1997; Jokat et al., 1996). It is probably a continuation of the Precambrian East Antarctica. Towards the basin, the middle layer in the crust disappears, whereas the lower crust exhibits the P-wave velocities between 7.1 and 7.4 km/s. The sediment thickness there reaches 14 km and the upper crust velocity decreases to 5.3–5.9 km/s (Fig. 3g). A more recent data from Shen et al. (2018) covered an area of the Filchner-Ronne Ice Shelf near the Ellsworth and Transantarctic Mountains. They provided the shear wave velocity model with 3.5–3.6, 3.6–3.7 and 3.8–4.3 km/s. For the Ellsworth-Whitmore Mountains region, Shen et al. (2018) listed the shear wave velocity 3.5–3.6, 3.6–3.7 and 3.8–4.0 km/s for the upper, middle and lower crust. Their S-velocity model agrees with O'Donnell

Fig. 4. Results of a seismic data interpolation and their comparison: (a) map of the consolidated crustal thickness. (b) Differences in the total crustal thickness between our and CRUST1.0 model.

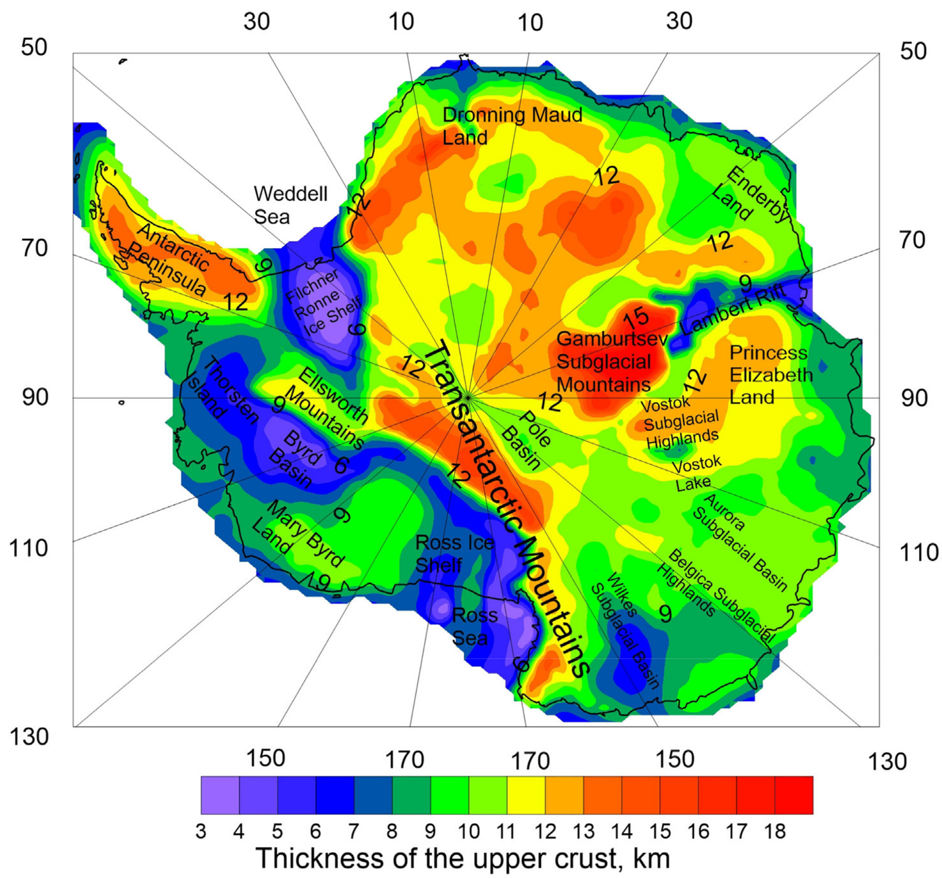
Dronning Maud Land
Weddell Sea
Enderby Land
Antarctic Peninsula
Filchner Ronne Ice Shelf
Lambert Rift
Gamburtsev Subglacial Mountains
Princess Elizabeth Land
Thorsten Island
Ellsworth Mountains
Transantarctic Mountains
Vostok Subglacial Highlands
Pole Basin
Byrd Basin
Vostok Lake
Aurora Subglacial Basin
Mary Byrd Land
Ross Ice Shelf
Belgica Subglacial Highlands
Wilkes Subglacial Basin
Ross Sea
3 4 5 6 7 8 9 10 11 12 13 14 15 16 17 18
Thickness of the upper crust, km

a

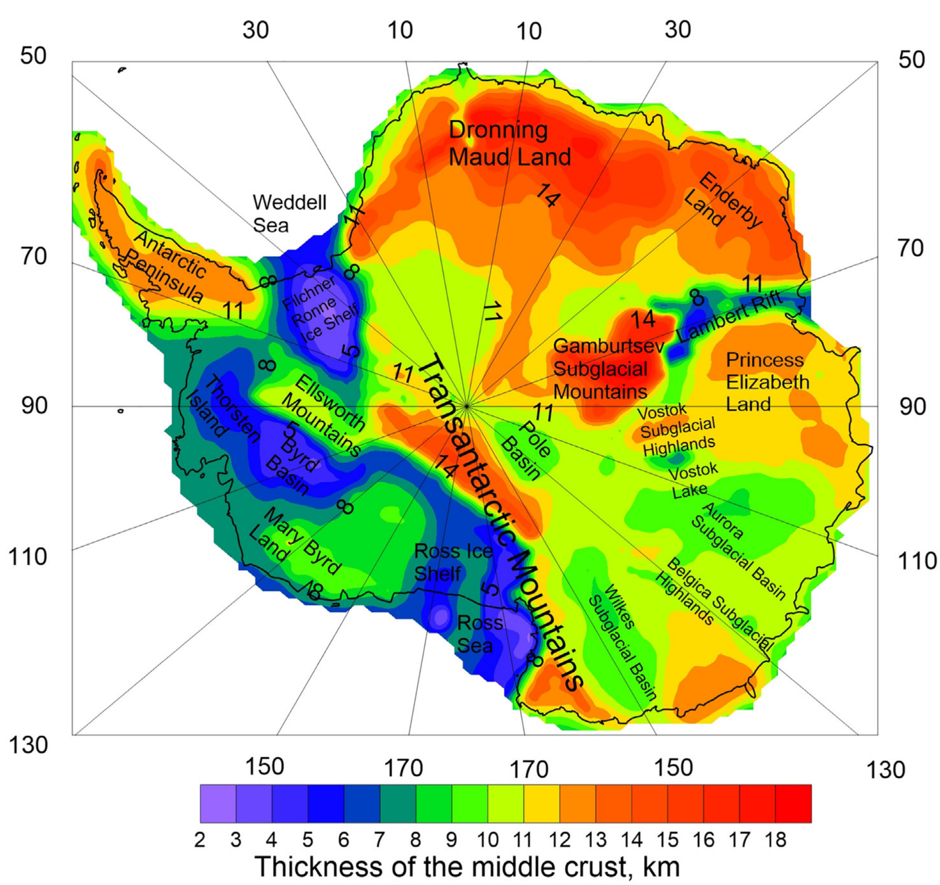
Dronning Maud Land
Weddell Sea
Enderby Land
Antarctic Peninsula
Filchner Ronne Ice Shelf
Lambert Rift
Gamburtsev Subglacial Mountains
Princess Elizabeth Land
Thorsten Island
Ellsworth Mountains
Transantarctic Mountains
Vostok Subglacial Highlands
Pole Basin
Byrd Basin
Vostok Lake
Aurora Subglacial Basin
Mary Byrd Land
Ross Ice Shelf
Belgica Subglacial Highlands
Wilkes Subglacial Basin
Ross Sea
2 3 4 5 6 7 8 9 10 11 12 13 14 15 16 17 18
Thickness of the middle crust, km

b

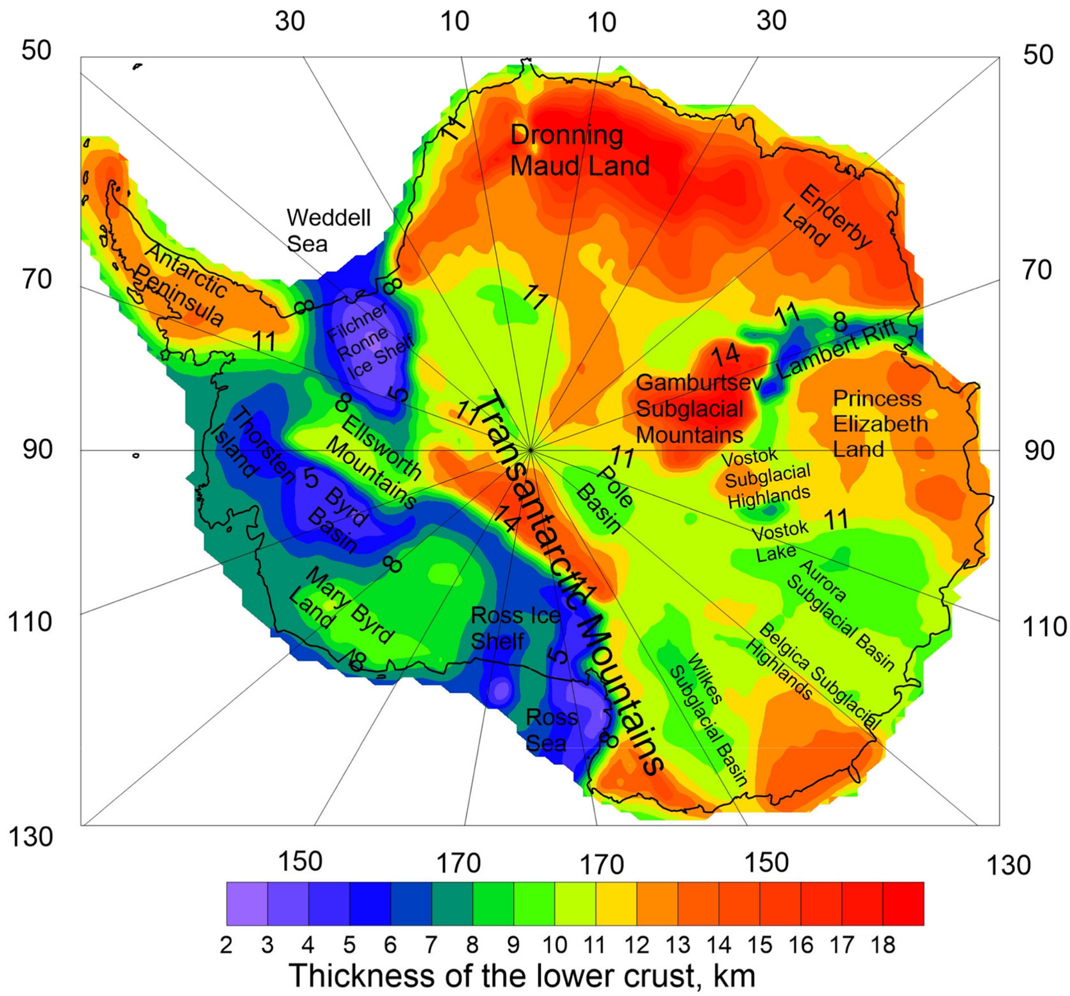

c

Fig. 6. Maps of the consolidated crust thickness for: the upper (a), middle (b) and lower (c) layers.

et al. (2019). Fig. 3h shows the average S-wave velocity profile for the Ellsworth-Whitmore Mountains.

4.3. Transantarctic Mountains

Along the Transantarctic Mountains border, the S-wave velocity changes in the range 3.5–3.6, 3.6–3.8 and 3.8–4.0 km/s for the upper, middle and lower crust (Shen et al., 2018). For parts of the Transantarctic Mountains near the coast of the Ross Sea the SRFs data from Pyle et al. (2010) provide similar values (Fig. 3i).

4.4. Bentley seismic profiles

Most of seismic profiles lie in coastal areas. However, there are three long seismic profiles across central parts of Antarctica (Bentley, 1973). Unfortunately, these profiles contain information only about the P-wave velocity in the upper crust and sediments. The profile AA′ begins at the base of the Antarctic Peninsula (6.0 km/s in the upper crust), passes along the western edge of the Ellsworth Mountains (6.1 km/s), continues through the Transantarctic Mountains near the South Pole (6.7 km/s) and terminates in the central part of the Dronning Maud Land (6.2–6.4 km/s). The section BB′ also starts at the base of the Antarctic Peninsula (6.0 km/s), crosses the Bentley Depression (5.9 km/s), the Marie Byrd Land, the Ross Ice Shelf (6.4 km/s), the Transantarctic Mountains (6.5 km/s), the Wilkes Basin and terminates in the Belgica Subglacial Highlands (5.8 km/s). The third CC′ seismic profile begins from the coast of the Amundsen Sea, crosses the Marie Byrd Land (6.1 km/s) and the Bentley Depression (5.9 km/s) and continues to the Transantarctic Mountains (6.7–7.0 km/s).

5. Results

Seismic data (summarized in Section 4) were used to compile the consolidated crustal model and P-wave velocities for the Antarctic continental crust. Results are presented in the following of this section.

5.1. Consolidated crustal model

We constructed maps of the consolidated crust thickness and inner crustal structure for each tectonic block. The consolidated crustal thickness is shown in Fig. 4a. Due to a large sediment accumulation in some parts of the continent, we recognized the existence of large differences between the Moho depth and consolidated crustal thickness, most remarkably beneath the Ronne Ice Shelf. The Moho deepens there to 26–30 km, while the consolidated crust is only 12–20 km thick due to the presence of a large basin with the 8–14 km sediment thickness. A stretched basement of continental origin forms the bottom of this basin. The same situation occurs in another wide area of a continental extension beneath the Ross Sea. The consolidated crustal thickness there varies from 10 to 22 km, but the sedimentary cover is much thinner (1–7 km). Except for the Antarctic Peninsula (30–38 km), the Marie Byrd Land (26–30 km) and the Ellsworth-Whitmore Mountains (32–34 km), a strongly thinned consolidated crust is detected throughout West Antarctica. Regions with a thinned consolidated crust in East Antarctica were identified beneath the Wilkes Subglacial Basin (26–30 km), the Lambert Rift (18–24 km), the Vostok Basin (24–28 km), the Belgica Subglacial Highlands (30–36 km), the Aurora Subglacial Basin (28–30 km) and the South Pole region (30–36 km). In contrast, a thickened consolidated crust in East Antarctica was found under the Gamburtsev Subglacial Mountains (44–58 km), the Wohlthat Massif (44–50 km) and the Kottas Mountains (44–50 km). Other regions in East Antarctica have a normal continental crust. The Transantarctic Mountains have a normal continental crust (34–38 km), except for its central part with a thickened crust (40–46 km). A comparison of our results with the global seismic crustal model CRUST1.0 reveals some notable differences (Fig. 4b).

Histograms of the consolidated crustal thickness individually for the Transantarctic Mountains, East Antarctica, West Antarctica and for the whole continent are plotted in Fig. 5. The average crustal thickness of West Antarctica is 24 km (with a standard deviation (STD) of 7.2 km) due to broad regions of a stretched crust. The average crustal thickness beneath the Transantarctic Mountains is 36 km (STD of 5.2 km). This value is typical for platforms but not for elevated orogens. The average crustal thickness of East Antarctica is 35 km (STD 5.7 km) due to broad regions with a stretched crust. The average crustal thickness for the whole continent is 31 km (STD 7.8 km).

Using seismic data and numerical techniques described above, we obtained thickness estimates for all three consolidated crustal layers at each point. Results are presented in Fig. 6.

As seen in Fig. 6a, the upper crustal thickness is typically 12–16 km. This value is specific for central parts of East Antarctica (Indo-Antarctica block), the Transantarctic Mountains and the Antarctic Peninsula. A thick upper crust (up to 18 km) was found beneath the Gamburtsev Mountains. Elsewhere in East and West Antarctica, we see a thin upper crust. A very thin upper crust was detected under the Ronne Ice Shelf, the Ross Sea, the Lambert Rift and the Byrd Basin (4–8 km). As seen in Fig. 6b, a thick middle crust (14–18 km) is mostly associated with orogens in East Antarctica. A thick middle crust was also found under the Enderby Land, while other orogens have a normal (Antarctic Peninsula and Transantarctic Mountains) or thin middle crust (Ellsworth Mountains). We identified a thin middle crust (less than 10 km) everywhere in West Antarctica, except for the Antarctic

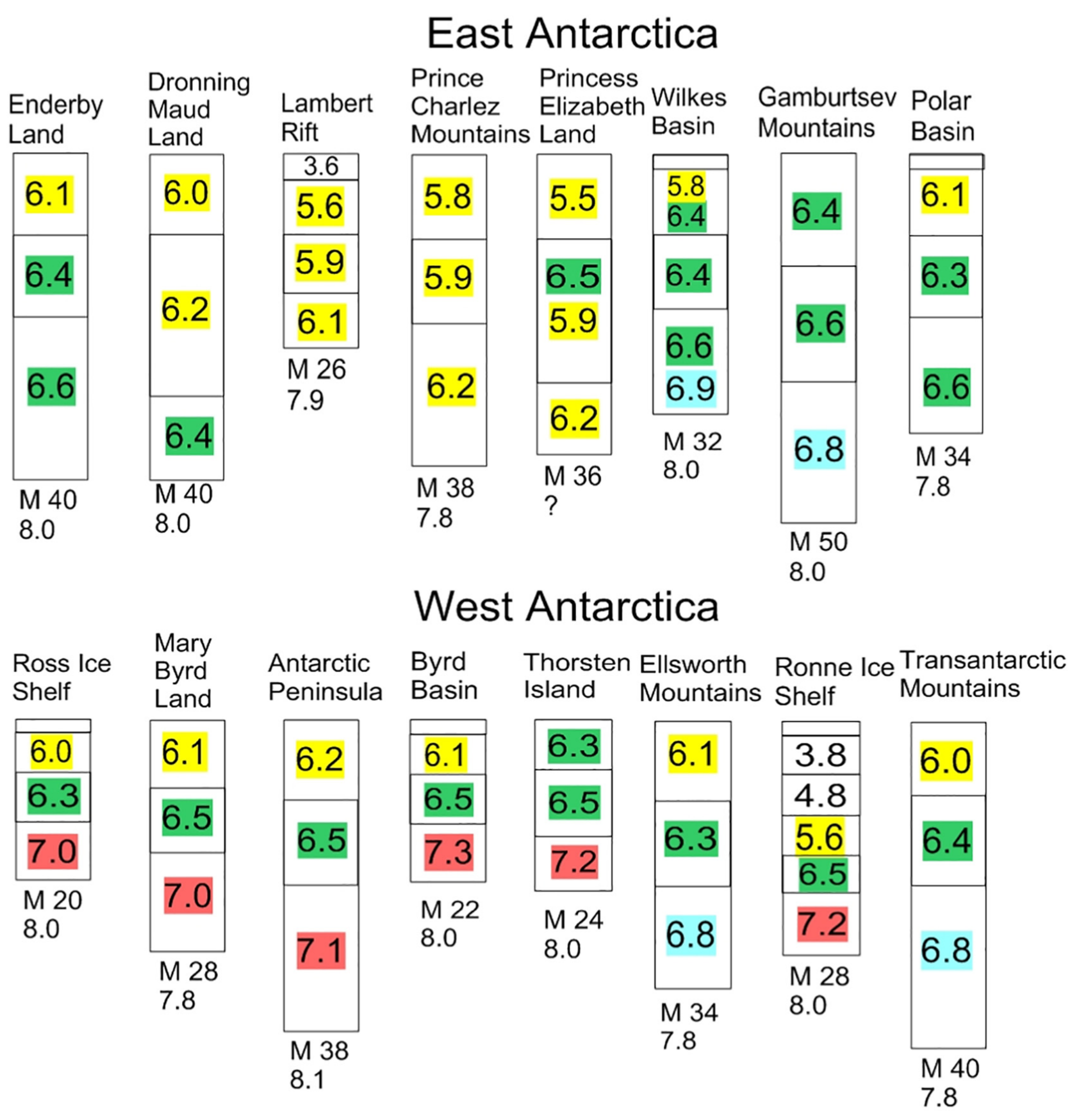

Fig. 7. The P-wave velocity diagrams of Antarctica.

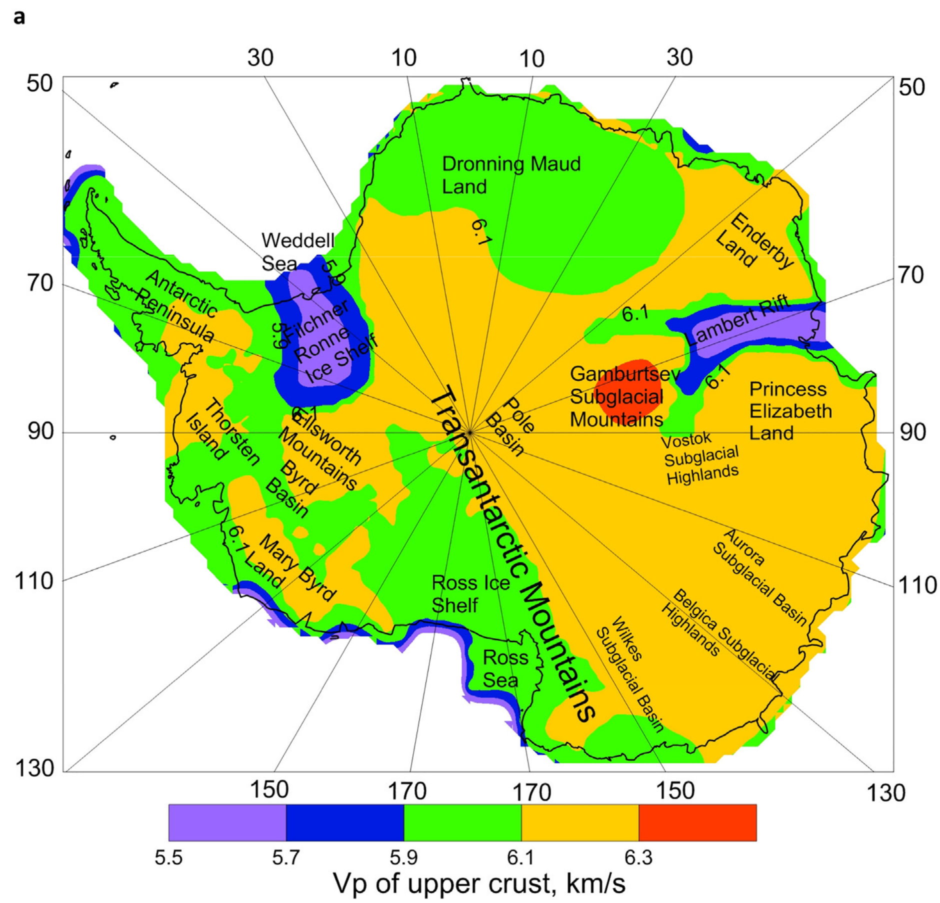
a
Dronning Maud Land
Weddell Sea
Antarctic Peninsula
Filchner Ronne Ice Shelf
Enderby Land
Lambert Rift
Gamburtsev Subglacial Mountains
Pole Basin
Transantarctic Mountains
Princess Elizabeth Land
Vostok Subglacial Highlands
Thorsten Island
Ellsworth Mountains
Byrd Basin
Mary Byrd Land
Ross Ice Shelf
Ross Sea
Aurora Subglacial Basin
Belgica Subglacial Highlands
Wilkes Subglacial Basin
5.5
5.7
5.9
6.1
6.3
Vp of upper crust, km/s

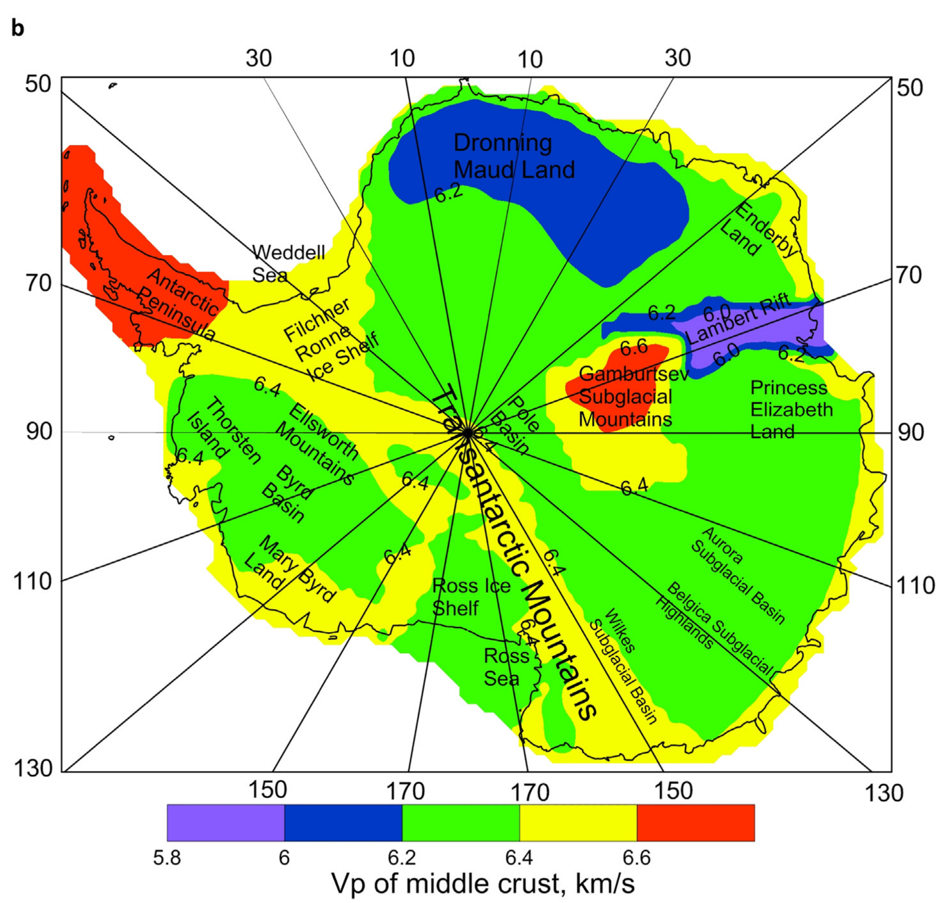
b
Dronning Maud Land
Weddell Sea
Antarctic Peninsula
Filchner Ronne Ice Shelf
Enderby Land
Lambert Rift
Gamburtsev Subglacial Mountains
Pole Basin
Transantarctic Mountains
Princess Elizabeth Land
Thorsten Island
Ellsworth Mountains
Byrd Basin
Mary Byrd Land
Ross Ice Shelf
Ross Sea
Aurora Subglacial Basin
Belgica Subglacial Highlands
Wilkes Subglacial Basin
5.8
6
6.2
6.4
6.6
Vp of middle crust, km/s

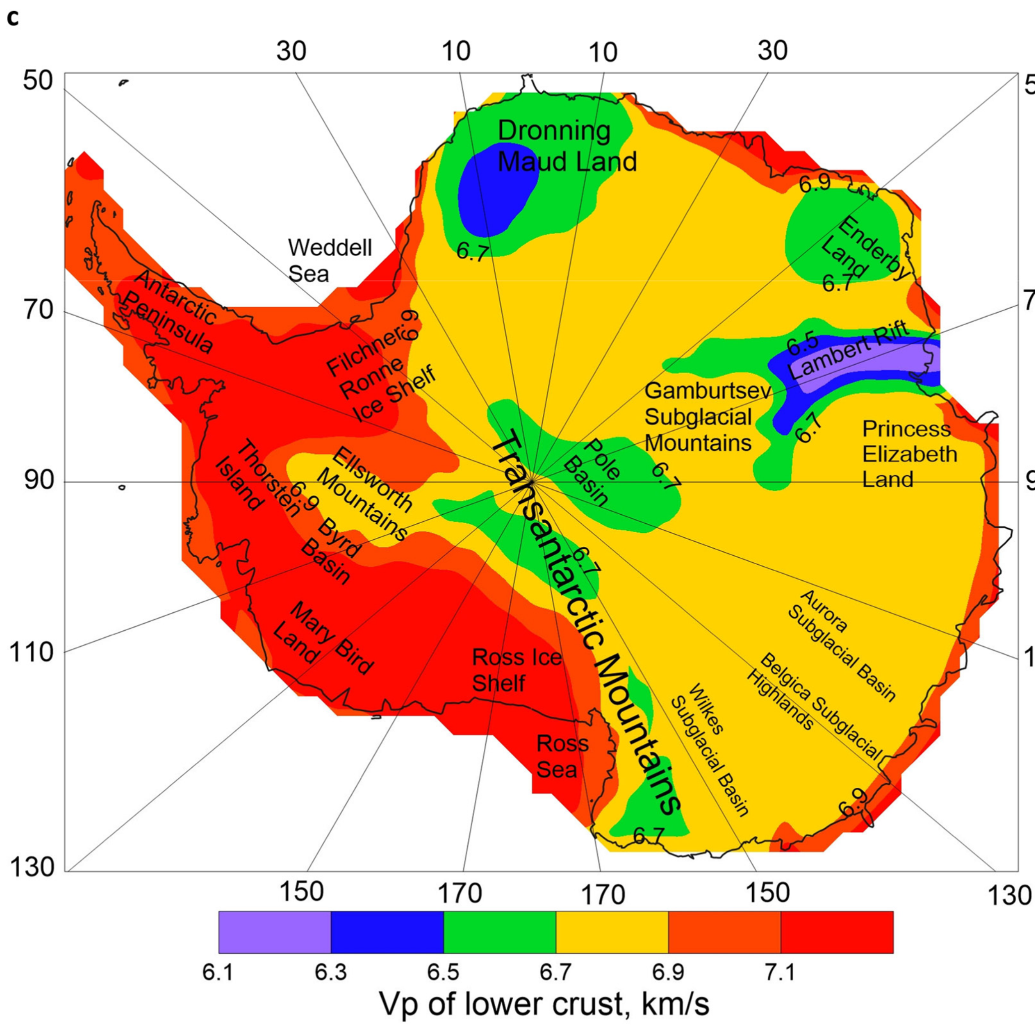

Fig. 8. Maps of the P-wave velocities in the upper (a), middle (b) and lower (c) consolidated crust.

Peninsula, the Marie Byrd Land and subglacial basins situated in East Antarctica. As seen in Fig. 6c, a thick lower crust lies under the Gamburtsev Mountains and orogens of the Dronning Maud Land (16–18 km). A thin crust is found under the Wilkes, South Pole and Aurora Basins, the Vostok depression and the Lambert Rift. In West Antarctica, a thin lower crust is present everywhere, except for the Antarctic Peninsula. The Transantarctic Mountains have normal lower crust, except for a thick crust in its central part. From the comparison of Fig. 6a-c, we see that the thickness of upper, middle and lower consolidated crustal layers generally correlate well with each other.

5.2. Velocity model

In Fig. 7, we show the average P-wave velocity profiles for different tectonic structures in Antarctica. The Lambert Rift, the Marie Byrd Land and the Ronne Ice Shelf have roughly the same Moho depth (26–28 km) but large velocity differences. We suggest that the Lambert Rift is an extension of stable Proterozoic crust, whereas the Marie Byrd Land and the Ronne Ice Shelf are rather young terranes with possible magmatic intrusions in the lower crust. For West Antarctica, lower crustal velocities are larger than expected for a normal continental crust. This finding indicates the presence of a predominantly mafic crustal composition (Christensen and Mooney, 1995), while the P- and S-wave velocities in the lower crust of East Antarctica are rather low (Table 2). This is the principal difference in the deep structure of these regions.

The P-wave velocity model for the Antarctic continent is shown in Fig. 8 (see also Table 2). Fig. 8a shows the P-wave velocity in the upper (consolidated) crust. A low velocity is observed beneath the Lambert Rift including surrounding regions (5.4–5.6 km/s) and the Filchner-Ronne Ice Shelf (5.3–5.9 km/s). The P-wave velocities in the middle crust are shown in Fig. 8b. A low velocity is detected beneath the Lambert Rift, including surrounding regions (5.8–5.9 km/s) and the Dronning Maud Land (6.1–6.2 km/s). The main part of Antarctica has a normal seismic velocity in the middle crust (6.2–6.5 km/s). The Antarctic Peninsula and the Gamburtsev Subglacial Mountains have a high velocity in the middle crust up to 6.7 km/s. Fig. 8c shows the P-wave velocity in the lower crust. A high velocity is usual for terranes in West Antarctica (Table 2), particularly under the Ross Ice Shelf (6.9–7.1 km/s), the Marie Byrd Land (7.0–7.4 km/s), the Antarctic Peninsula (7.2–7.3 km/s) and the Filchner-Ronne Ice Shelf (7.1–7.4 km/s). The Transantarctic, Gamburtsev and Ellsworth-Whitmore Mountains have an intermediate velocity in the lower crust (6.8 km/s). We detected rather low velocities in East Antarctica beneath the Dronning Maud Land (6.4 km/s) and the Lambert Rift, including surrounding regions (6.1–6.2 km/s). Compared to CRUST1.0, our model revealed more details in the pattern of seismic velocities. Extensive regions characterized by similar velocities, in agreement with CRUST1.0, split into separated structures (see Fig. 8a-c). High velocities in the lower crust in West Antarctica can be explained by a crustal stretching and magmatic underplating. In the stable Precambrian crust of East Antarctica with a strong and cold lithosphere (e.g., Morelli and Danesi, 2004), the velocity is low. The P-wave velocity in crustal layers generally tends to increase with depth. A particular feature of the seismic velocity distribution in the crust is the presence of a low-velocity zone. We identified such zone beneath the Princes Elizabeth Land, specifically a low-velocity layer at depths ~20–25 km (5.8–5.9 km/s).

6. Discussion and concluding remarks

We analysed different geophysical data involving the subglacial bedrock relief, the Moho depth, the consolidated crustal and sediment thickness and seismic velocities in the crust to update the model of the Antarctic crustal structure. For this purpose, we also collected information from seismic profiles that had never been published in the English literature. According to our results, the geological structure of this continent can be categorized as follows: West Antarctica represents a large area of a stretched continental crust with age of rocks from Neoproterozoic to Cenozoic. It contains deep sedimentary basins of the Ross Ice Shelf (up to 6 km), the Ronne Ice Shelf (up to 14 km) and the Bentley Depression (4–6 km). The Transantarctic Mountains and the Ellsworth-Whitmore Mountains have shallow orogenic roots that do not ensure their isostatic compensation and perhaps the same origin. East Antarctica is formed by rocks with age from Archean to Early Palaeozoic. It is not just a simple Precambrian platform, because it includes different crustal blocks. East Antarctica embrace the broad sedimentary basins of the Aurora, South Pole, Wilkes and Vostok Basins and the Lambert Depression, with sediment thickness up to ~6 km. Rifts continue from the coast to the South Pole region. According to the subglacial bedrock relief, the East Antarctic Rift System is roughly 2500 km long. The crustal thickness varies from 10 to 20 km along the West Antarctic Rift System, up to 50 km under mountain ranges in East Antarctica. Diagrams of the crustal thickness revealed that the main peak lies within the range 30–32 km. These values correspond to broad areas of a thin crust in East Antarctica. For all continents, the average crustal thickness is ~31 km. We constructed the three-layer consolidated crust model for tectonic blocks using data from seismic profiles, SRFs, ambient noise and the BEDMAP2 bedrock relief dataset. As an initial model of crustal thickness we used the previous ANTMoho model. We then interpreted results by means of the type and origin of these crustal blocks. Our final model consists of maps, providing information about the Moho depth, the total consolidated crustal thickness, the sediment thickness and the P-wave velocity of the upper, middle and lower consolidated crustal layers. According to the P-wave velocity profiles, we concluded that in the Precambrian crust of East Antarctica, a mafic layer in the lower consolidated crust is absent. Low velocities characterize this crust, whereas young extended crust of West Antarctica has a thick mafic layer with the P-wave velocity in the range 7.0–7.3 km/s. A high velocity in the lower crust for West Antarctica terranes can be interpreted as underplating with magma accumulations during a crustal extension or as the result of a mantle plume activating (e.g., Danesi and Morelli, 2001; Faccenna et al., 2008; An et al., 2015). For the Princess Elizabeth Land, we found a low-velocity layer at depths ~20–25 km (5.8–5.9 km/s). The velocities in the upper mantle under the Moho interface are rather uniform: ranging 7.8–8.1 km/s for West Antarctica and 7.8–8.0 km/s for East Antarctica. Principal differences exist between the East and West Antarctic Rift Systems. The latter is a wide active rift with an ongoing extension and broad and deep sedimentary basins. The West Antarctic Rift System is characterized by high P-and S-wave velocities in the lower crust detected under all tectonic blocks except for the Ellsworth-Whitmore and Transantarctic Mountains. The middle crust beneath the Filchner-Ronne Ice Shelf is likely absent. We speculate that the East Antarctic Rift System is an extension of old Precambrian crust with low P-wave velocities. Currently, this rift system is passive, narrower while also comprising thinner sedimentary basins if compared to the West Antarctic Rift System. Low velocities also indicate that the magmatism and underplating under the East Antarctic Rift System are absent.

These results confirmed a significant contrast between the crustal structures of East and West Antarctica. The crustal structure of East Antarctica is dominated by normal or slightly thinned crustal layers. In West Antarctica, the crustal layers are mostly thin, except under the Antarctic Peninsula. A thick lower crust and orogenic roots were detected beneath the Gamburtsev Mountains and orogens of the Dronning Maud Land. Elsewhere, mountains ranges including also the Transantarctic Mountains are without the presence of significant crustal roots. According to seismic data, the thickness of upper, middle and lower crustal layers usually correlate with each other. We found large crustal variations for Antarctica using seismic and other geophysical data and sufficiently improved the CRUST1.0 crustal model of Antarctica. This information is essential for better understanding of processes and history of the amalgamation and separation of Gondwana. Nevertheless, new seismic data are still needed particularly in central part of East Antarctica.

Declaration of competing interest

The authors declare that they have no known competing financial interests or personal relationships that could have appeared to influence the work reported in this paper.

Acknowledgements

We thank Anya M. Reading and an anonymous reviewer for constructive comments which helped to improve the manuscript significantly. This work was carried out within the framework of the state assignment of the IPE RAS.

CRediT authorship contribution statement

AB designed and performed calculations of the maps, provided a main framework of the research.

RT provided a tectonic scheme and corrected the manuscript.

AM provided a general leadership and corrected the manuscript.

References

Aitken, A.R.A., Young, D.A., Ferraccioli, F., Betts, P.G., Greenbaum, J.S., Richter, T.G., Roberts, J.L., Blankenship, D.D., Siegert, M.J., 2014. The subglacial geology of Wilkes Land, East Antarctica. Geophys. Res. Lett. 41, 2390–2400.

An, M., Wiens, D.A., Zhao, Y., Feng, M., Nyblade, A.A., Kanao, M., Lévêque, J.J., 2015. S-velocity model and inferred Moho topography beneath the Antarctic Plate from Rayleigh waves. Journal of Geophysical Research: Solid Earth 120 (1), 359–383.

Baranov, A., 2010. A new crustal model for Central and Southern Asia. Izvest Phys Solid Earth 46, 34–46.

Baranov, A., Bobrov, A., 2018. Crustal structure and properties of Archean cratons of Gondwanaland: similarity and difference. Russ. Geol. Geophys. 59, 512–524.

Baranov, A., Morelli, A., 2013. The Moho depth map of the Antarctica region. Tectonophysics 609, 299–313.

Baranov, A., Tenzer, R., Bagherbandi, M., 2018. Combined gravimetric-seismic crustal model for Antarctica. Surv. Geophys. 39 (1), 23–56.

Bassin, C., Laske, G., Masters, G., 2000. The current limits of resolution for surface wave tomography in North America. EOS Trans AGU 81, F897.

Bayer, B., Geissler, W., Eckstaller, A., Jokat, W., 2009. Seismic imaging of the crust beneath Dronning Maud Land, East Antarctica. Geophys. J. Int. 178, 860–876.

Behrendt, J.C., Le Masurier, W.E., Cooper, A.K., Tessensohn, F., Trehu, A., Damaske, D., 1991. Geophysical studies of the West Antarctic rift system. Tectonics 10 (6), 1257–1273.

Bentley, C., 1973. Crustal structure of Antarctica. Tectonophysics 20, 229–240.

Bentley, C., 1991. Configuration and structure of the subglacial crust. In: Tingey, R.J. (Ed.), The Geology of Antarctica Clarendon. Oxford, U. K, pp. 335–364.

Block, A.E., Bell, R.E., Studinger, M., 2009. Antarctic crustal thickness from satellite gravity: implications for the transantarctic and Gamburtsev Subglacial Mountains. Earth Planet. Sci. Lett. 288, 194–203.

Boger, S.D., 2011. Antarctica—before and after Gondwana. Gondwana Res. 19, 335–371.

Boger, S., Wilson, C., 2003. Brittle faulting in the Prince Charles Mountains, East Antarctica: cretaceous transtensional tectonics related to the break-up of Gondwana. Tectonophysics 367, 173–186.

Chaput, J., Aster, R.C., Huerta, A., Sun, X., Lloyd, A., Wiens, D., Nyblade, A., Anandakrishnan, S., Winberry, J.P., Wilson, T., 2014. The crustal thickness of West Antarctica. J. Geophys. Res. Solid Earth https://doi.org/10.1002/2013JB010642.

Chisenga, C., Yan, J., Yan, P., 2019. A crustal thickness model of Antarctica calculated in spherical approximation from satellite gravimetric data. Geophys. J. Int. 218 (1), 388–400.

Christensen, N.I., Mooney, W.D., 1995. Seismic velocity structure and composition of the continental crust: a global view. J. Geophys. Res. 100 (B7), 9761–9788.

Dalziel, I.W.D., 1992. Antarctica: a tale of two supercontinents. Annu. Rev. Earth Planet. Sci. 20, 501–526.

Dalziel, I.W.D., Elliot, D.H., 1982. West Antarctica; problem child of Gondwanaland. Tectonics 1 (1), 3–19.

Danesi, S., Morelli, A., 2001. Structure of the upper mantle under the Antarctic Plate from surface wave tomography. Geophys. Res. Lett. 28, 4395–4398.

Faccenna, C., Rossetti, F., Becker, T.W., Danesi, S., Morelli, A., 2008. Recent extension driven by mantle upwelling at craton edge beneath the Admiralty Mountains (Ross Sea, East Antarctica). Tectonics 27. https://doi.org/10.1029/2007TC002197.

Ferraccioli, F.F., Coren, E., Bozzo, C., Zanolla, S., Gandol, I., Tabacco, E., Frezzotti, M., 2001. Rifted crust at the East Antarctic Craton margin: gravity and magnetic interpretation along traverse across the Wilkes Subglacial Basin region. Earth Planet. Sci. Lett. 192, 407–421.

Ferraccioli, F., Finn, C., Jordan, T., Bell, R.E., Anderson, L.M., Damaske, D., 2011. East Antarctic rifting triggers uplift of the Gamburtsev Mountains. Nature 479, 388–392. https://doi.org/10.1038/nature10566.

Filina, I., Blankenship, D., Thoma, M., Lukin, V., Masolov, V., Sen, M., 2008. New 3D bathymetry and sediment distribution in Lake Vostok: implication for pre-glacial origin and numerical modeling of the internal processes within the lake. Earth Planet. Sci. Lett. 276 (1–2), 106–114.

Fitzsimons, I.C.W., 2000. A review of tectonic events in the East Antarctic Shield and their implications for Gondwana and earlier supercontinents. J. Afr. Earth Sci. 31 (1), 3–23.

Fretwell, P., Pritchard, H.D., Vaughan, D.G., Bamber, J.L., Barrand, N.E., Bell, R., Bianchi, C., Bingham, R.G., Blankenship, D.D., Casassa, G., Catania, G., Callens, D., Conway, H., Cook, A.J., Corr, H.F.J., Damaske, D., Damm, V., Ferraccioli, F., Forsberg, R., Fujita, S., Gogineni, P., Griggs, J.A., Hindmarsh, R.C.A., Holmlund, P., Holt, J.W., Jacobel, R.W., Jenkins, A., Jokat, W., Jordan, T., King, E.C., Kohler, J., Krabill, W., Riger-Kusk, M., Langley, K.A., Leitchenkov, G., Leuschen, C., Luyendyk, B.P., Matsuoka, K., Nogi, Y., Nost, O.A., Popov, S.V., Rignot, E., Rippin, D.M., Riviera, A., Roberts, J., Ross, N., Siegert, M.J., Smith, A.M., Steinhage, D., Studinger, M., Sun, B., Tinto, B.K., Welch, B.C., Young, D.A., Xiangbin, C., Zirizzotti, A., 2013. Bedmap2: improved ice bed, surface and thickness datasets for Antarctica. The Cryosphere Discuss. 6, 4305–4361.

Grad, M., Guterch, A., Janik, T., Sroda, P., 2002. Seismic characteristic of the crust in the transition zone from the Pacific Ocean to the northern Antarctic Peninsula. West Antarctica. Antarctica at the close of a millennium. Royal Society of New Zealand Bulletin. 35, 493–498.

Groenewald, P., Grantham, G., Watkeys, M., 1991. Geological evidence for a Proterozoic to Mesozoic link between southeastern Africa and Dronning Maud Land, Antarctica. J. Geol. Soc. Lond. 148, 1115–1123.

Hansen, S., Nyblade, A., Pyle, M., Wiens, D., Anandakrishnan, S., 2009. Using S wave receiver functions to estimate crustal structure beneath ice sheets: an application to the Transantarctic Mountains and East Antarctic craton. Geochem. Geophys. Geosyst. 10, Q08014.

Hansen, S., Nyblade, A., Heeszel, D., Wiens, D., Shore, P., Kanao, M., 2010. Crustal structure of the Gamburtsev Mountains, East Antarctica, from S-wave receiver functions and Rayleigh wave phase velocities. Earth Planet. Sci. Lett. 300, 395–401.

Hansen, S., Kenyon, L., Graw, J., Park, Y., Nyblade, A., 2016. Crustal structure beneath the Northern Transantarctic Mountains and Wilkes Subglacial Basin: implications for tectonic origins. J. Geophys. Res. Solid Earth 121, 812–825.

Hole, M.J., LeMasurier, W.E., 1994. Tectonic controls on the geochemical composition of Cenozoic, mafic alkaline volcanic rocks from West Antarctica. Contrib. Mineral. Petrol. 117, 187–202.

Hungeling, A., Tyssen, F., 1991. Reflection seismic measurements in western Neuschwabenland. In: Thornson, M.R.A., Crame, J.A., Thomson, J.W. (Eds.), Geological Evolution of Antarctica. Proceedings of the Fifth International Symposium on Antarctic Earth Sciences. Robinson College, Cambridge, Cambridge University Press, Cambridge, UK, p. 73.

Isanina, E., Krupnova, N., Popov, S., Masolov, V., Lukin, V., 2009. Deep structure of the Vostok Basin, East Antarctica as deduced from seismological observations. Geotektonika 3, 45–50.

Jacobs, J., Fanning, C.M., Henjes-Kunst, F., Olesch, M., Paech, H.J., 1998. Continuation of the Mozambique Belt into East Antarctica: Grenville-age metamorphism and polyphaser Pan-African high-grade events in central Dronning Maud Land. J. Geol. 106 (4), 385–406.

Jacobs, J., Bauer, W., Fanning, C.M., 2003. Late Neoproterozoic/Early Palaeozoic events in central Dronning Maud Land and significance for the southern extension of the East African Orogen into East Antarctica. Precambrian Res. 126, 27–53.

Jokat, W., Miller, H., Hübscher, C., 1996. Structure and origin of southern Weddell Sea crust: results and implications. Geology Society, London. Spec. Publ. 108, 201–211.

Kalberg, T., Gohl, K., 2014. The crustal structure and tectonic development of the continental margin of the Amundsen Sea Embayment, West Antarctica: implications from geophysical data. Geophys. J. Int. 198, 327–341.

Kanao, M., Fujiwara, A., Miyamachi, H., Toda, S., Tomura, M., Ito, K., Ikawa, T., 2011. Reflection imaging of the crust and the lithospheric mantle in the Lutzow-Holm Complex, Eastern Dronning Maud Land, Antarctica, derived from the SEAL Transects. Tectonophysics 508, 73–84.

Kennett, B.L.N., Engdahl, E.R., 1991. Travel times for global earthquake location and phase association. Geophys. J. Int. 105, 429–465.

Kogan, A., 1971. First experience in crustal investigation for Antarctica by deep seismic sounding. Russ. Geol. Geophys. 10, 84–89 (in Russian).

Kolmakov, A., Mishenkin, B., Solovyev, D., 1975. Deep seismic studies in East Antarctica. Bull. Soviet Antarc. Exped. 5–15 (in Russian).

Kriegsman, L.M., 1995. The Pan-African event in East Antarctica: a view from Sri Lanka and the Mozambique Belt. Precambrian Res. 75, 263–277.

Laske, G., Masters, G., Ma, Z., Pasyanos, M.E., 2013. Update on CRUST1.0—a 1-degree global model of Earth's crust. Geophys Res Abstr 15:2658.

Lawrence, J.F., Wiens, D.A., Nyblade, A., Anandakrishnan, S., Shore, P.J., Voigt, D., 2006. Crust and upper mantle structure of the Transantarctic Mountains and surrounding regions from receiver functions, surface waves, and gravity: implications for uplift models. Geochem Geophys Geosyst 7.

Leitchenkov, G., Kudryavtzev, G., 1997. Structure and origin of the Earth's Crust in the Weddell Sea Embayment (beneath the Front of the Filchner and Ronne Ice Shelves) from deep seismic sounding data. Polarforschung 67 (3), 143–154.

Lisker, F., Brown, R., Fabel, D., 2003. Denudation and thermal history along a transect across the Lambert Graben, northern Prince Charles Mountains, Antarctica, derived from apatite fission track thermochronology. Tectonics 22, 1055.

Llubes, M., Florsch, N., Legresy, B., Lemoine, J.M., Loyer, S., Crossley, D., Remy, F., 2003. Crustal thickness in Antarctica from CHAMP gravimetry. Earth Planet. Sci. Lett. 212, 103–117.

Llubes, M., Seoane, L., Bruinsma, S., R'emy, F., Geodesy, P., 2017. Crustal thickness of Antarctica estimated using data from gravimetric satellites. Solid Earth 1–26.

McGinnis, L.D., Bowen, R.H., Erickson, J.M., Allred, B.J., Kreamer, J.L., 1985. East-West Antarctic boundary in McMurdo Sound. Tectonophysics 114, 341–356.

Mikhalsky, E.V., 2008. Age of the Earth's crust and the Nd isotopic composition of the mantle sources of East Antarctic complexes. Geochem. Int. 46 (2), 168.

Morelli, A., Danesi, S., 2004. Seismological imaging of the Antarctic continental lithosphere: a review, Global Planet. Change 42, 155–165.

O'Donnell, J.P., Nyblade, A.A., 2014. Antarctica's hypsometry and crustal thickness: implications for the origin of anomalous topography in East Antarctica. Earth Planet. Sci. Lett. 388, 143–155.

O'Donnell, J.P., Brisbourne, A.M., Stuart, G.W., Dunham, C.K., Yang, Y., Nield, G.A., Whitehouse, P.L., Nyblade, A.A., Wiens, D.A., Anandakrishnan, S., Aster, R.C., Huerta, A.D., Lloyd, A.J., Wilson, T., Winberry, J.P., 2019. Mapping crustal shear wave velocity structure and radial anisotropy beneath West Antarctica using seismic ambient noise. Geochem. Geophys. Geosyst. 20 (11), 5014–5037.

Pappa, F., Ebbing, J., Ferraccioli, F., 2019. Moho depths of Antarctica: comparison of seismic, gravity, and isostatic results. Geochem. Geophys. Geosyst. 20, 1629–1645.

Pyle, M.L., Wiens, D.A., Nyblade, A.A., Anandakrishnan, S., 2010. Crustal structure of the Transantarctic Mountains near the Ross Sea from ambient seismic noise tomography. Journal of Geophysical Research: Solid Earth. 115 (B11).

Ramirez, C., Nyblade, A., Emry, E.L., Julià, J., Sun, X., Anandakrishnan, S., Wiens, D.A., Aster, R.C., Huerta, A.D., Winberry, P., Wilson, T., 2017. Crustal structure of the Transantarctic Mountains, Ellsworth Mountains and Marie Byrd Land, Antarctica: constraints on shear wave velocities, Poisson's ratios and Moho depths. Geophys. J. Int. 211 (3), 1328–1340.

Reading, A., 2004. The seismic structure of Wilkes Land/Terre Adelie, East Antarctica and comparison with Australia: first steps in reconstructing the deep lithosphere of Gondwana. Gondwana Res. 7, 21–30.

Reading, A., 2006. The seismic structure of Precambrian and early Paleozoic terranes in the Lambert Glacier region East Antarctica. Earth Planet. Sci. Lett. 244, 44–57.

Rino, S., Kon, Y., Sato, W., Maruyama, S., Santosh, M., Zhao, D., 2008. The Grenvillian and Pan-African orogens: world's largest orogenies through geologic time, and their implications on the origin of superplume. Gondwana Res. 14, 51–72.

Rudnick, R.L., Fountain, D.M., 1995. Nature and composition of the continental crust: a lower crustal perspective. Rev. Geophys. 33, 267–310.

Shen, W., Wiens, D.A., Anandakrishnan, S., Aster, R.C., Gerstoft, P., Bromirski, P.D., et al., 2018. The crust and upper mantle structure of central and West Antarctica from Bayesian inversion of Rayleigh wave and receiver functions. Journal of Geophysical Research: Solid Earth 123, 7824–7849.

Straume, E.O., Gaina, C., Medvedev, S., Hochmuth, K., Gohl, K., Whittaker, J.M., et al., 2019. GlobSed: Updated total sediment thickness in the world's oceans. Geochem. Geophys. Geosys. 20.

Studinger, M., Bell, R., Buck, W., Karner, G., Blankenship, D., 2004. Subglacial geology inland of the TransantarcticMountains in light of new aerogeophysical data. Earth Planet. Sci. Lett. 220, 391–408.

Tarkov, A., Vavakin, V., 1982. Poisson's ratio behavior in various crystalline rocks: application to the study of the Earth's interior. Phys. Earth Planet. Inter. 29, 24–29.

ten Brink, U.S., Hackney, R.I., Bannister, S., Stern, T.A., Makovsky, Y., 1997. Uplift of the Transantarctic Mountains and the bedrock beneath the East Antarctic ice sheet. J. Geophys. Res. 102, 27,603–27,621.

Trey, H., Cooper, A., Pellis, G., della Vedova, B., Cochrane, G., Brancolini, G., Makris, J., 1999. Transect across the West Antarctic rift system in the Ross Sea, Antarctica. Tectonophysics 301, 61–74.

Winberry, P., Anandakrishnan, S., 2004. Crustal structure of the West Antarctic rift system and Marie Byrd Land hotspot. Geology 977–980.

Wörner, G., 1999. Lithospheric dynamics and mantle sources of alkaline magmatism of the Cenozoic West Antarctic Rift system. Glob Planet Change 23, 61–77.

Zhu, L., Kanamori, H., 2000. Moho depth variation in Southern California from teleseismic receiver functions. J Geophys Res 105, 2969–2980.